NAVIGATING THE COSTS OF MOVEMENT: CHARACTERIZING ENERGY EXPENDITURE DURING LONG-DISTANCE FORAGING IN GREATER SPEAR-NOSED BATS

By

Travis David Bayer

A Thesis Submitted to the Faculty
of Southeastern Louisiana University
in Partial Fulfillment of the Requirements
for the Degree of Master of Science
In Biology

Southeastern Louisiana University
Hammond, Louisiana

August 2024

Copyright by
Travis David Bayer
2024

NAVIGATING THE COSTS OF MOVEMENT: CHARACTERIZING ENERGY EXPENDITURE DURING LONG-DISTANCE FORAGING IN GREATER SPEAR-NOSED BATS

By

Travis David Bayer

Approved:

M. Teague O'Mara, Ph.D.
Adj. Asst. Prof. of Biological Sciences
Director Of Conservation Evidence
Bat Conservation International
(Director of Thesis)

Christopher K. Beachy, Ph.D.
Professor of Biological Sciences
(Committee Member)

Christopher M. Murray, Ph.D.
Associate Prof. of Biological Sciences
(Committee Member)

Justin R. Anderson, Ph.D.
Department Head of the Department
of Biological Sciences

Daniel R. McCarthy, Ph.D.
Dean of the College of Science and Technology

Name: Travis David Bayer

Previous Degrees: B.S., Minnesota State University, 2021, (Zoology)

Date of Current Degree: July 25, 2024

Institution: Southeastern Louisiana University

Major Field: Biological Sciences (Movement Ecology)

Major Professor: Dr. M. Teague O'Mara

Title of Study: NAVIGATING THE COSTS OF MOVEMENT: CHARACTERIZING ENERGY EXPENDITURE DURING LONG-DISTANCE FORAGING IN GREATER SPEAR-NOSED BATS

Pages in Study: 104

Candidate for Degree of Master of Science

Energy use is at the center of adaptation and evolution. To be successful, individuals must manage their energy expenditure and intake. One method of measuring this in free-living wildlife has been to measure where the animals go using GPS, and how much they move using tri-axial accelerometers. This combination has been shown to be highly correlated with energy expenditure in birds and many terrestrial mammals. However, the complex kinematics of bat flight may make acceleration-based proxies for energy expenditure less accurate than in other taxa. Because bats live at their energetic ceiling, understanding their energy expenditure and how to accurately measure it is key to testing fundamental hypotheses about their evolution and success, including decision-

making, physiological adaptation, movement patterns, and sociality. To test if energy expenditure is predicted by accelerometer-based movement in bats, we deployed heart rate loggers alongside GPS with tri-axial accelerometers on 11 free-roaming greater spear-nosed bats (*Phyllostomus hastatus*) on Isla Colón in Panamá. We used heart rate-based estimates of energy expenditure to develop relationships between vectorial dynamic body acceleration (VeDBA) and estimated energy expenditure. We detailed how these energy proxies interact with an additional metric of energy expenditure, airspeed. These relationships are then used to show movement-based energy landscapes – or the distribution of energy expenditure over space and time. Calibrated energy landscapes provide perspectives that allow for the exploration of how and why individual bats make movement-based decisions. Given both have been used as proxies for energy use, we hypothesized that heart rate would positively reflect increases in VeDBA and that information on behavior would further detail this relationship. Because airspeed is an important predictor of metabolic flight requirements, we also hypothesized that bats would primarily fly within energetically optimal range flight speeds. Plots of airspeed and flight duration showed that the majority of all flights were flown within energetically-optimal airspeeds. When modeling the relationship between VeDBA and airspeed, our models also reflected previously established mechanical power curve estimates for this species. We found VeDBA to have a strong positive relationship with heart rate, and that our models moderately increased when behavioral states of flying vs resting were defined. We conclude that VeDBA measured from free-flying bats predicts energy

expenditure, measured through multiple metrics, and information on behavior can provide improved accuracy of energy expenditure estimates.

Key Words: tri-axial accelerometry, heart rate, airspeed, energy expenditure, vectorial dynamic body acceleration, energy distribution, energy landscape

DEDICATION

I would like to dedicate this research to my best friend, Jax. Seven years and two degrees later, we did it together.

ACKNOWLEDGEMENTS

I want to thank my advisor, Dr. Teague O'Mara for teaching me everything I know about a subject I have become so passionate about. Over the past two years, I have learned more than I ever imagined possible. Thank you for believing in me, showing me independence and work ethic, and helping me grow both as a researcher and as a person. You have taught me skills in research design, data analysis, and scientific communication that I will carry with me throughout my career. Working with you has given me the best possible graduate school and field experience. This project has been more than I could have ever asked for, and I feel incredibly lucky to have been a part of it.

I want to also thank my co-advisor and committee member, Dr. Christopher Beachy, for taking me into his lab and treating me as one of his own students. I am grateful for all I have been able to learn from you during your lab meetings, and for all the career advice you have provided. You're wrong about Godzilla (1998).

Thank you to my committee member Dr. Christopher Murray. You have made my lectures as well as graduate school enjoyable, while always emphasizing the importance of rigorous science and research. Your guidance and encouragement have been invaluable throughout this journey. Croc on.

Thank you, Maggie, my biggest support system. You've stood by me through all the highs and lows, always with a smile. I couldn't have done this without you.

Lastly, thank you to the bats, the central focus of this study. They served as the perfect winged subjects to teach me fundamental lessons in a complex topic, but also just as much about life and myself.

TABLE OF CONTENTS

LIST OF TABLES

LIST OF FIGURES

CHAPTER I

INTRODUCTION

Ecological and Evolutionary Significance of Energy Expenditure

Energy serves as the currency of life. It influences nearly every aspect of biology and behavior.

Animals have a finite amount of energy available to maximize their fitness (Brown et al., 2004; Hicks et al., 2017; Jeanniard-du-Dot et al., 2017b), and are often faced with trade-offs between survival and reproduction as a result of this energetic constraint on life history (Brown et al., 2004; Halsey et al., 2009; Hicks et al., 2017; Jeanniard-du-Dot et al., 2017b; Rebstock et al., 2022; Weimerskirch et al., 2003). Managing the balance between energy intake and expenditure is crucial for their survival, and influences behaviors that maximize food intake while minimizing expenditure (Anholt and Werner, 1995; Monteith et al., 2013, Scacco, 2021). Studying the movements and physiology of animals offers insights into how animals navigate the complex challenges posed by their energy requirements (Bishop et al., 2015; Elliott et al., 2013; Nathan et al., 2008; Shepard et al., 2013). Understanding these metabolic trade-offs and the role of energy allocation in wildlife ecology and evolution is fundamental to explaining the relationship between ecosystem dynamics and the adaptations of species to their environments (Nathan et al., 2008). This requires effective methods to measure or estimate energy distribution across different behaviors and time

scales (Shepard et al., 2013; Wilson et al., 2012). However, quantifying energy expenditure in free-living animals can be challenging.

Unique to each animal is their energy distribution, which comprises two major processes; intake and expenditure. An animal's energy intake refers to their acquisition of energy through food consumption, while their energy expenditure encompasses the various ways in which they spend their energy, including locomotion, thermoregulation, body maintenance, and reproduction. Energy expenditure influences life history traits, such as growth rates, reproductive output, and survival (Jeanniard-du-Dot et al., 2017b; Pontzer and McGrosky, 2022; Robertson et al., 2016; Sansom et al., 2009; Stephens and Krebs, 1986; Watanabe et al., 2020; Weimerskirch et al., 2003). Changes in the amount of energy that is allocated towards these different activities reflects adaptive responses to environmental conditions and evolutionary pressures (Auer et al., 2020; Kordas et al., 2022; McGrosky and Pontzer, 2023). Reproduction is an energetically intensive biological process. Therefore, energy expenditure is a crucial determinant of individual fitness, helping shape population dynamics (Brown et al., 2004; Halsey et al., 2009; Hicks et al., 2017; Jeanniard-du-Dot et al., 2017b; Rebstock et al., 2022; Smallegange et al., 2016; Weimerskirch et al., 2003).

Species exhibit remarkable flexibility in energy allocation, adjusting metabolic rates and behavioral decisions in response to new ecological pressures (Bozinovic et al., 2007; Cant et al., 1996; Geiser, 2004; Geiser, 1988; Martins, 2024; Niven and Laughlin, 2008; Sabat et al., 1995; Schramski et al.,

2015; Stearns, 1998). The interaction between energy intake and expenditure drives ecological interactions and can shape evolutionary trajectories (Algar et al., 2007; Andrewartha, and Birch, 1954; Kearney, 2012; Tomlinson et al., 2014). For instance, predator-prey dynamics are influenced by the energetic costs incurred by the predator from hunting, and the energetic costs incurred by the prey from avoiding predation (Bro-Jørgensen, 2013; Brose et al., 2008; Dawkins and Krebs, 1979; Janzen, 1980; Scales et al., 2009; Wilson et al., 2018). These ecological and physiological demands surrounding energy distribution can lead to selective pressure on physiologies that influence the rate at which energy is expended (Bro-Jørgensen, 2013; Scales et al., 2009; Simpson, 1944; Wilson et al., 2018).

The evolutionary arms race between the cheetah and impala has driven the co-evolution of speed (Bro-Jørgensen; Wilson et al., 2018; Wilson et al., 2013). Selective pressures from cheetah predation spurred the evolution of faster impalas over generations. In tandem, cheetahs also experienced similar pressures, favoring speed (Wilson et al., 2018). Slower individuals were likely gradually eliminated, favoring the evolution of increased speed in both species. Strategies for energy expenditure can target the optimization of morphologies (Dickinson et al., 2000). A cheetah has the ability to accomplish high speeds due in part to its increased hindlimb length (Hudson et al., 2011), hindlimb shape (Andersson & Werdelin, 2003), shoulder and spine flexibility (Meachen et al., 2018), wide nostrils with enlarged nasal passages, semi-retractable claws (Gray, 1968; Meachen et al., 2018), muscle fiber composition (Williams et al., 1997) and

optimal body size (Hirt et al., 2017). Furthermore, the co-evolution between predator and prey has been detailed in the relationships between lions - zebras, and cheetahs - impalas (Wilson et al., 2018). Using muscle biopsies and GPS & IMU collars to track location, acceleration, and body posture, biomechanical profiles of predator-prey interactions were developed, which detailed the strategies used by predators and prey to either capture prey or evade predators (Wilson et al., 2018). The results showed that lions and cheetahs had increased speed, muscle power, and capacity to accelerate and decelerate than their prey. These advantages were matched by the increased turning maneuverability of zebras and impalas compared to their predators (Wilson et al., 2018). The physiological capabilities of lions and cheetahs for pursuit, and of zebras and impalas for escape has resulted in sustainable success rates for both, demonstrating how the evolution of one species, predator or prey, can influence the evolution of the other (Bro-Jørgensen, 2013; Wilson et al., 2018).

Physiological traits for energy distribution can also encompass variation in organ size (Bozinovic et al., 2007; Canals et al., 2005). The Chilean mouse opossum exhibits strong phenotypic flexibility in organ size. In times of food scarcity, these opossums are capable of reducing the size of energetically expensive organs like the digestive tract and liver, enabling them to maintain positive energy balances (Bozinovic et al., 2007).

Bats are another example of an animal that possesses a diversity of physiological changes which aid in their locomotion. An example of this is seen in the heart and lung size in bats. As a result of the increased energetic cost that

flight demands, bats exhibit the largest relative heart and lung size compared to any other mammal with a heart to body ratio of 1.37% compared to 0.6% of most other mammals (Canals et al., 2005). Bats also display a significantly higher red blood cell count ($11.0 \cdot 10^6$-$26.2 \cdot 10^6$ RBC/gml) compared to other mammals ($8.8 \cdot 10^6$–$18.3 \cdot 10^6$ RBC/gml) (Jürgens et al., 1981). These changes enable them to achieve larger blood oxygen capacities, which allow for higher specific oxygen uptake (Jürgens et al., 1981). The size, shape, and morphological characteristics of a bat's wing corresponds to their diet, mode of flight, and environment (Norberg and Rayner, 1987). Increased maneuverability and low wing loading (mass/wing area) is favored in insectivorous species gleaning in dense forests and is often correlated with short, broad wings, and short, rounded wing tips. Higher flight speeds and wing loading is ideal for insectivores hunting in more open habitats, often correlating with longer and narrower wings. Nectarivorous bats often have short wing spans allowing them to fly close to flowers, but large wing tips which are valuable for providing lift while hovering at low speeds (Norberg and Rayner, 1987).

Animals exhibit diverse physiological traits and foraging strategies to acquire energy resources efficiently (Canals et al., 2005; Dickinson et al., 2000; Jürgens et al., 1981; Norberg, 2021; Norberg and Rayner, 1987; Reichle, 2023; Stephens and Krebs, 1986; Wilkinson & Boughman, 1998; Wilson et al., 2018). Increased foraging efficiency can positively influence energy distribution through increasing the reliability of energy intake and decreasing the time and energy spent looking for food (Brose et al., 2008; Parker et al., 1996; Stephens and

Krebs, 1986; Weimerskirch et al., 2003). Selection should favor foraging efficiency and success (Frey-Roos et al., 1995; Jeanniard-du-Dot et al., 2017b; Lescroël et al., 2010; Rebstock et al., 2022; Reichle, 2023; Robertson et al., 2016; Watanabe et al., 2020). Animals are then faced with trade-offs between energy acquisition and expenditure, balancing the benefits of high-energy foods against the costs of obtaining them (Stephens, and Krebs, 1986). Knowledge of how much energy is distributed among these processes should prove important to understanding their movement decisions and overall ecology.

A number of methods of quantifying energy expenditure have been developed (Green 2011, Wilson et al 2006, Butler et al 2004, Hicks et al 2017, Sutton et al 2023), but much of this work has relied on captive use in a laboratory setting. Less invasive methods have been developed that use dynamic body acceleration of an animal as a proxy for energy expenditure. Vectorial Dynamic Body Acceleration (VeDBA) has shown high accuracy across various taxa (Bidder et al., 2017; Elliott et al., 2013; Jeanniard-du-Dot et al., 2017a; Ladds et al., 2017; Metcalfe et al., 2016; Miwa et al., 2015; Mori et al., 2015; Qasem et al., 2012; Rezende et al., 2023; Stothart et al., 2017; Sutton et al., 2023; Sutton et al., 2021; Udyawer et al., 2017; Wilson et al., 2020; Wright et al., 2014). However, its reliability in animals with complex locomotion kinematics or those moving through viscous or resistant mediums remains uncertain due to its strong reliance on terrestrial estimates of acceleration-based energy expenditure (Wilson et al., 2020). Verification of VeDBA is necessary to ensure it accurately reflects energy expenditure, considering factors like species locomotion styles

and environmental interactions. These challenges are highlighted by diving sea birds, which not only fly through the air column, but also navigate water. While diving, dynamic body acceleration was shown to have a different relationship with energy expenditure than during flight (Elliott et al., 2013; Gómez Laich et al., 2011; Hicks et al., 2017). Muscle efficiency can differ with different modes of locomotion and the medium being traversed (Gómez Laich et al., 2011). This means that the relationship between oxygen consumption and accelerometry may differ in each case (Elliott et al., 2013; Gómez Laich et al., 2011; Hicks et al., 2017). Without validation, there is substantial risk of errors in estimating energy expenditure, potentially leading to inaccurate conclusions about animal behavior, ecology, and energy budgets. Accurate understanding of an animal's energy distribution is necessary for assessing the costs of behaviors like foraging, migration, and dispersal, which are essential for survival in many species (Masello, et al., 2021; Scacco, 2021; Scacco et al., 2019; Shepard et al., 2013; Williams and Safi, 2021; Wilson et al., 2012). It also reveals how environmental changes and human activities affect animal populations, and offers insights into their adaptability (Horstkotte et al., 2023; Mandel and Bildstein, 2007; Masello et al., 2021; Monteith et al., 2018; Shaw, 2020; Shepard et al., 2013; Wang et al., 2017).

Methods of Measuring Energy Expenditure

All behavior is tied to an energetic cost, and understanding the cost framework gives a fundamental window into behavioral decision-making (Shepard et al., 2013; Wilson et al., 2012).

Doubly labeled water provides a comprehensive measure typically over a 24-hour period, useful for understanding daily energy expenditure (Speakman and Racey, 1988; Speakman, 1997). Flow-through respirometry measures instantaneous metabolic rates during short-term activities, offering insights into immediate energy demands (Lighton and Halsey, 2011). Heart rate monitoring provides a continuous assessment of immediate energy expenditure, particularly beneficial for quick bursts of behavior (Barkse et al., 2014). Tri-axial accelerometry offers fine-scale, continuous data on movement patterns and activity levels over seconds to minutes, enabling detailed assessments of energy expenditure during specific behaviors (Shepard et al., 2008).

Doubly Labeled Water

The doubly labeled water (DLW) method has been shown to serve as a good measure for the amount of energy an animal spends between two defined times (Butler et al., 2004; Nagy et al., 1999; Speakman, 1997; Speakman, 1998; Sutton et al., 2021; Westerterp, 2017). This method uses a baseline collection of an animal's urine or saliva, followed by orally administering $^{2}H_{2}{}^{18}O$ (doubly labeled water). A final saliva sample is collected hours later with a urine sample the

following day. The results of DLW are based on differential elimination of isotopes from the body as H_2O or $H_2O + CO_2$. Using the animal's fluid samples, CO_2 production can be calculated. While using DLW has been shown to provide highly accurate energy estimates, is less invasive, and unobtrusive, and are only provided with a single, time-averaged estimate of oxygen consumption ($\dot{V}O_2$) (Speakman, 1997; Speakman, 1998) without any information about frequency or intensity. Both active (e.g., foraging) and resting energy comprise energy expenditure and can be measured across short- and long-term scales (Elliott et al., 2016; Green, 2011; Green et al., 2008; Green et al., 2009; Halsey et al., 2009; Speakman, 1997; Speakman, 1998). Although DLW can provide a value for daily energy expenditure, it cannot measure its composition or how it's distributed (Speakman, 1997; Speakman, 1998).

Flow-through Respirometry

Further work has been built on metabolic measurements within a tightly controlled laboratory setting using flow-through respirometry (FTR) (Lighton and Halsey, 2011). Here, the animal is placed into a chamber for a defined period of time and oxygen is pumped through at a set flow rate. This technique also utilizes oxygen consumption ($\dot{V}O_2$) as a proxy for energy expenditure and is based on the idea that the amount of oxygen consumed and carbon dioxide produced can be measured from the concentration of each gas in the incurrent and excurrent airstreams with respect to flow rates.

While these measures (DLW, FTR) have been shown to be accurate in a variety of taxa (Enstipp et al., 2011; Geiser et al., 2019; McNab and Weston, 2018; Payne et al., 2015; Speakman and Racey, 1988; Westerterp, 2017), they cannot completely replicate every environmental condition and their respective energy costs. Furthermore, subsequent studies have shown that estimations of energy expenditure in captivity may be inaccurate as different behaviors come with different energetic costs and the behaviors seen in a controlled environment do not reflect those exhibited in free-living animals (Bishop and Spivey, 2015; Bowlin et al., 2005).

Heart Rate

Since each heart beat transports oxygen in blood to working tissues throughout the body, measurements of an animal's heart rate can provide information on how much energy is being expended, and for how long through estimating the oxygen needed to generate energy for a behavior and duration of time (Bishop and Spivey, 2013; Brown et al., 2022; Butler et al., 2004; Green, 2011; Green et al., 2008).

When allometrically scaled with respect to a particular species, heart rate has a proportional relationship with blood flow and oxygen consumption at each level of cardiac work (Bishop and Spivey, 2013; Brown et al., 2022; Butler et al., 2004; Green, 2011; Green et al., 2008). Each beat of the heart delivers oxygen to the rest of the body to be used for the generation and expenditure of energy. By measuring heart rate frequency, energy expenditure can be determined through

estimating that rate of oxygen consumption by tissues during sustained movement (Barske et al., 2014; Bishop et al., 2015; Bishop and Spivey, 2013; Brown et al., 2022; Butler et al., 2004; Bowlin and Wikelski, 2008; Green, 2011; Green et al., 2008; O'Mara et al., 2017). This concept relies on the Fick principle that relates the total uptake of oxygen ($\dot{V}O_2$) to cardiac output (heart rate * stroke volume) and arteriovenous O_2 difference (Bishop and Spivey, 2013). The arteriovenous difference represents the amount of oxygen being delivered to specific working tissue and is expressed as the difference of oxygen being carried in the arteries and in the veins. The rate of oxygen consumption by working tissue is dependent on the volume of blood being pumped to the tissue and the efficiency at which the tissue can extract oxygen from the blood. This establishes a relationship between heart rate and oxygen consumption, which can then be converted to kilojoules (kJ min^{-1}) (Bishop and Spivey, 2013; O'Mara et al., 2017).

Estimating Energy Expenditure in the Field

Accelerometry

An animal responds to its environment through an alteration in its behavior (Shepard et al., 2008). Behavior can often be characterized by the animal's body posture and motion, or the static and dynamic components (Shepard et al., 2013; Shepard et al., 2008). For example, a bat's flight is characterized by movement with a horizontal body posture, but while roosting its body is in a vertical orientation from head to tail. These are aspects that are measurable by recording

an individual's acceleration in all three-dimensions (O'Mara et al., 2019; Shepard et al., 2008). In terms of total acceleration, the variation in velocity as a direct result of an animal's movement is its dynamic acceleration. This metric can be obtained using a body-mounted triaxial accelerometer attached to the trunk of an animal and a basic understanding of physics (Shepard et al., 2008). These devices work by simultaneously measuring acceleration in three orthogonal axes (**Figure 1 | a**); sway (x), surge (y), and heave (z) (O'Mara et al., 2019; Shepard et al., 2008). Based on Newton's 3rd law, when an animal moves a limb in one direction, there will be a corresponding opposite and equal movement in the trunk (Shepard et al., 2008). This is easily noticeable in movement such as bat flight (**Figure 1 | b**). The more repetitive the motion (such as wingbeats), the more apparent this change in dynamic acceleration becomes (O'Mara et al., 2019; Shepard et al., 2008). The power stroke from a downwards wingbeat will result in the body of the bat moving in the opposite upward direction with an equal force (Kato et al., 2006; Shepard et al., 2008). This change in the trunk's dynamic acceleration, in any dimension, is measurable when the animal is outfitted with a dorsally-attached accelerometer (Shepard et al., 2008).

These data can then estimate energy expenditure based on the principle that movement will typically cause a greater increase in energy expenditure than any other process (Elliott et al., 2013; Spivey and Bishop, 2013; Stothart et al., 2016; Wilson et al., 2020). Tri-axial accelerometers can also capture locomotor detail such as limb cycling or wing beat frequency (Bishop et al., 2015; O'Mara et al., 2019; Shepard et al., 2008), as well as behavioral activity profiles (Brown et

al., 2019; Shepard et al., 2008), as well as behavioral activity profiles (Brown et al., 2013; Chakravarty et al., 2019; Patterson, 2019).

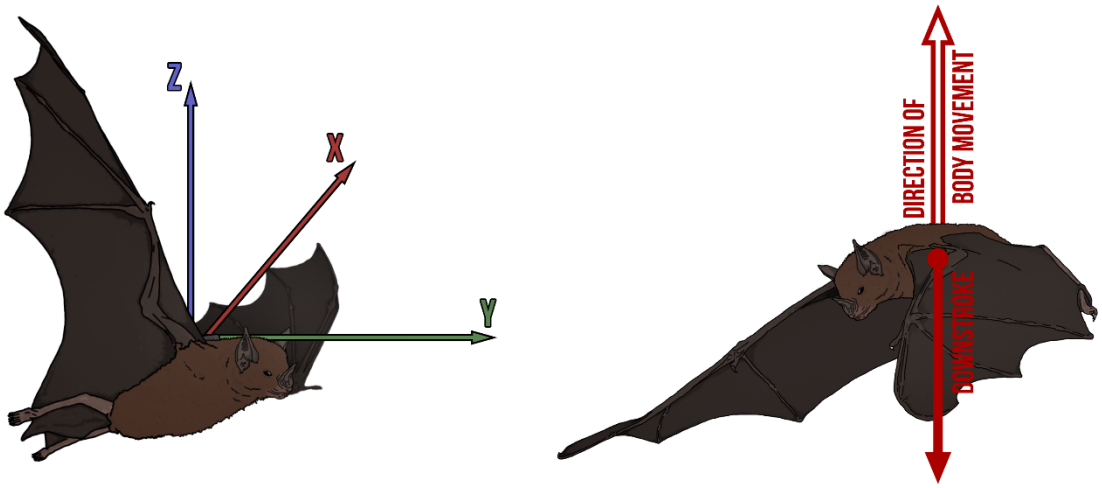

Figure 1. (a) Illustration of a greater spear-nosed bat outfitted with a tri-axial accelerometer. Each arrow represents a measurable axis of acceleration. The labeling order of axes is relative to our study and is dependent on the direction of tag placement. Red represents sway (X), green is surge (Y), and blue is heave (Z). **(b)** Depiction of bat flight demonstrating how the power of a downstroke creates an equal and opposite force moving the body in the opposite direction.

Different behaviors come at different energetic costs (Elliott et al., 2013; Gómez Laich et al., 2011; Hicks et al., 2017; Williams et al., 2014). Sprinting requires more energy than walking (Williams et al., 2014). Traveling up an incline costs more energy than on level ground (Dunford et al., 2020). The longer an intensive behavior is performed, the more energy it costs to sustain that behavior (Brown et al., 2023; Mills and Mills, 2017; Williams et al., 2014). When we account for what behavior an animal is performing and for how long, using what is known as a time-activity budget, we can increase the accuracy of our energy proxies (Brown et al., 2022; Elliott et al., 2013; Gómez Laich et al., 2011; Hicks et al., 2017; Jeanniard-du-Dot et al., 2017a, 2017c; Ladds et al., 2017; Wilson et al.,

2006). Time-activity budgets for different behaviors largely characterize the true nature of an animal's energy distribution but can be difficult to properly allocate without obtaining measurements from a free-living animal behaving under natural conditions (Brown et al., 2022; Jeanniard-du-Dot et al., 2017a, 2017c; Ladds et al., 2017). Ultimately, measuring energy expenditure in free-living animals provides a crucial method for understanding their physiological needs and ecological interactions (Brown et al., 2022; Green et al., 2009; Hicks et al., 2017; Nagy et al., 1999; Parker et al., 1996; Wilson et al., 2006). Unlike laboratory settings, field studies offer a natural environment where animals can exhibit normal behaviors without constraints. This natural context allows researchers to capture a more accurate representation of an animal's daily energy expenditure, as it encompasses the full range of activities such as foraging, hunting, and resting (Dunford et al., 2020; Williams et al., 2014). Importantly, field studies account for environmental variability, such as temperature, rain, and wind, as well as terrain, all of which significantly influence metabolic rates and the cost of travel (Dickinson et al., 2021).

Exploring Energy Estimates Using Heart Rate

The use of acceleration as a proxy for energy expenditure relies on the fact that most energy expenditure above resting metabolic rate is due to movement (King & Farner, 1961). However, acceleration metrics can represent poorer estimates of energy expenditure during processes like resting metabolic inactivity (Green et al., 2009; Hicks et al., 2017; Weimerskirch et al., 2016). The advantage of

measuring heart rate as a metric for energy expenditure is that you are provided not only with more accurate metabolic measures of activity, but also periods of rest and its associated metabolic activity (Bishop et al., 2015; Bishop and Spivey, 2013; Brown et al., 2022; Butler et al., 2004; Bowlin and Wikelski, 2008; Green, 2011; Green et al., 2008; O'Mara et al., 2017). Therefore, outfitting a free-living animal with heart rate loggers and tri-axial accelerometers enables a real-time examination of VeDBA estimates within their natural environment (Bishop et al., 2015; Brown et al., 2022; Green et al., 2008; Hicks et al., 2017; Miwa et al., 2015). By comparing changes in heart rate with corresponding fluctuations in VeDBA during different levels of activities under natural environmental conditions, we can assess the accuracy and reliability of VeDBA as an energetic proxy (Bishop et al., 2015). Paired with GPS, these estimations can be annotated at a behavioral, spatial, and temporal scale (**Figure 2**).

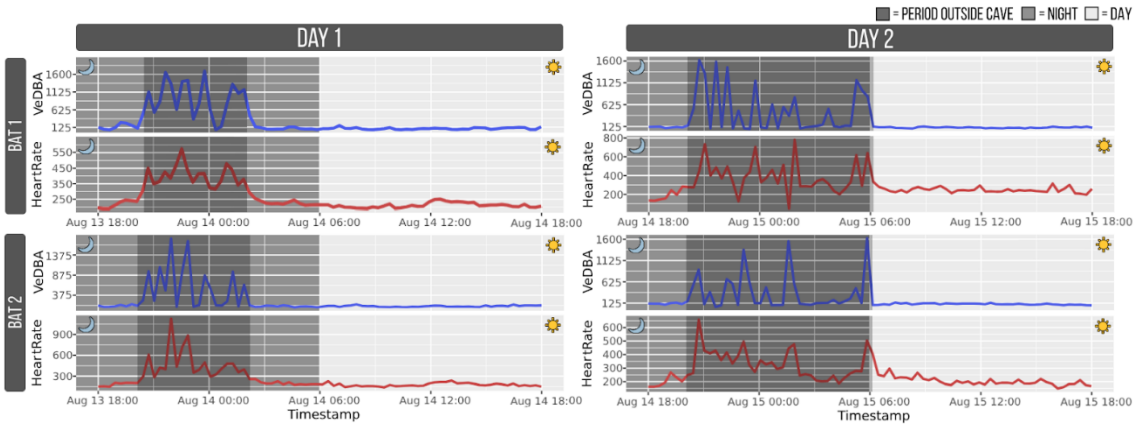

Figure 2. Vectorial dynamic body acceleration (VeDBA) (blue) and heart rate (red) for 2 bats plotted over two 24-hour periods, starting from 18:00:00 to 18:00:00. The light grey represents the daytime, darker grey represents nighttime, and the darkest grey represents the duration of time the bat was outside their cave.

In previous work, these same measures were collected on bar-headed geese (*Anser indicus*) during their annual migratory journey over the Himalayan mountains (Bishop et al., 2015). The study explored how these birds navigate one of the most challenging aerial routes, which involves crossing high mountain peaks that reach altitudes exceeding 5,000 meters. The study revealed that bar-headed geese adopt a "roller coaster" flight pattern, utilizing updrafts and thermals to gain altitude before gliding downhill, thereby minimizing their energy expenditure. Using GPS and a combination of tri-axial accelerometry and heart rate loggers, researchers were able to verify the use of VeDBA with these birds during flight by comparing them against the more established measure of energy expenditure, heart rate (Bishop et al., 2015).

Airspeed

Knowing the speed at which an animal travels is an ecologically significant metric that influences animal behavior, decision making, and the distribution of energy. During flight, speed is dependent on the mass and wing load of the animal (Bowlin and Wikelski, 2008; Hedenström and Alerstam, 1996; Hedenström and Thomas, 1995; Pennycuick, 2008; Pennycuick, 1975; Riskin et al., 2010). Changes to airspeed can be made by changing the frequency, angle, and amplitude of wingbeats (Ward et al., 2001).

How fast some animals fly has shown to be linked to their energy expenditure (Hedenström and Alerstam; 1996; Hedenström and Thomas, 1995;

O'Mara and Dechmann, 2023; Pennycuick, 2008; Pennycuick, 1975; von Busse et al., 2013). In birds, previous work has shown there to be strong curvilinear relationships between airspeed and the mechanical power needed to maintain that speed (Elliott et al., 2014; Hedenström and Alerstam, 1996; Hedenström and Thomas, 1995).

Aerodynamic theory predicts that during flight, energy expenditure is directly dependent on the speed of flight (Pennycuick, 2008; Pennycuick, 1975; Rayner, 1979; Tucker, 1974). These theories increase that dependence, especially during high and low airspeeds and wind speeds, showing an increase in the energy required to maintain flight during these times. This relationship of airspeed to energy expenditure (mechanical power) can be visualized through a simple power curve (**Figure 3**). Based on an animal's weight and the size and shape of its wings, the mechanical power needed to fly at a given speed follows a U or J-shaped curve (Hedenström and Alerstam; 1996; Hedenström and Thomas, 1995; O'Mara and Dechmann, 2023; Pennycuick, 2008; Pennycuick, 1975; von Busse et al., 2013). There is a minimum power speed (U_{mp}), or range of speeds that are the most economical for short distances. At speeds lower than U_{mp}, it becomes increasingly energetically costly to simply stay aloft due to increased power needed to generate lift. Similarly, above U_{mp}, increasing flight speed comes at increasing energetic costs due to increased drag of the faster-moving animal. The point at which the best possible ratio between power required to maintain level flight and speed to move long distances is indicated by the maximum range speed (U_{mr}) (Pennycuick, 2008; Pennycuick, 1975).

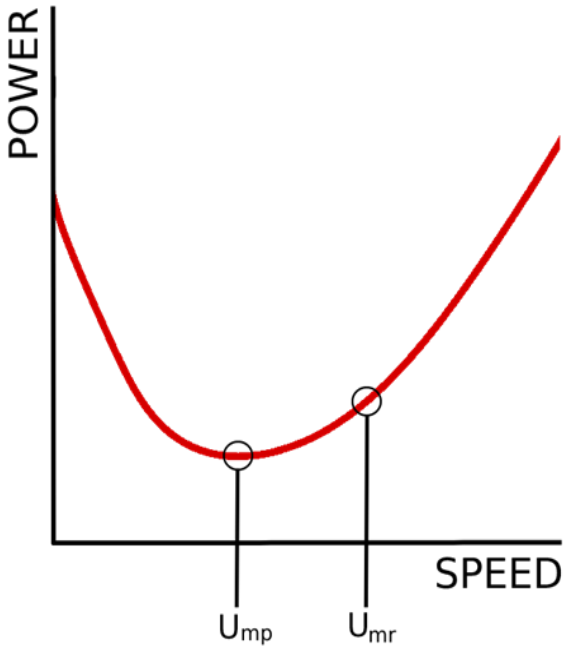

Figure 3. Standard model of animal flight power curve developed by Pennycuick, 2008. Minimum power speed is represented by U_{mp}, and maximum range speed by U_{mr}. Initially increasing speed (ms^{-1}) reduced the required power for flight as it is too energetically costly to stay aloft at extremely low flight speeds. Past U_{mp}, the required power for flight increases linearly with flight speed.

The predictability value of this model has been supported through a wide range of studies (Engel et al., 2010; Hedenström and Alerstam; 1996; Hedenström and Thomas, 1995; Pennycuick, 2008; Pennycuick, 1975; Tobalske et al., 2003), including work on several bat species (O'Mara & Dechmann, 2023; von Busse et al., 2013). The model implies that all animals capable of flight have a species-specific optimal flight speed. This optimal flight speed would lie at some point on the curve between U_{mp} and U_{mr}. The animal should then choose a flight speed as close as possible to optimal flight speed, relative to the task being performed and the benefit gained (O'Mara & Dechmann, 2023; von Busse et al., 2013).

Classifying Behavior With Accelerometry

Dynamic body acceleration is useful when trying to differentiate between transient behaviors or as a proxy of the energy spent for the duration of a particular behavior (Bishop et al., 2015; Hicks et al., 2017; O'Mara et al., 2019; Shepard et al., 2013; Shepard, 2008; Wilson et al., 2018; Williams et al., 2014). With an understanding of the animal's physics (Spivey and Bishop, 2013), body mechanics (O'Mara et al., 2019), and a basic understanding of their landscape and medium they travel through (Shepard et al., 2013), we can identify signatures in acceleration data characteristic of distinct behaviors (Hicks et al., 2017; O'Mara and Dechmann, 2022; Shepard et al., 2008; Williams et al., 2014) (**Figure 4**). The use of acceleration-based energy estimates and behavioral classification has shown promise in a variety of taxa and studies (Bidder et al., 2017; Elliott et al., 2013; Hicks et al., 2017; Jeanniard-du-Dot et al., 2017a; Ladds et al., 2017; Metcalfe et al., 2016; Miwa et al., 2015; Mori et al., 2015; O'Mara, et al., 2019; Qasem et al., 2012; Rezende et al., 2023; Shepard et al., 2013; Shepard et al., 2008; Stothart et al., 2017; Sutton et al., 2023; Sutton et al., 2021; Udyawer et al., 2017; Williams et al., 2014; Wilson et al., 2020; Wilson et al., 2012; Wright et al., 2014).

A previous study detailed hunting habits and preferences of pumas (*Puma concolor*) using a combination of GPS and tri-axial accelerometers (Williams et al., 2014). By identifying unique changes in the animal's acceleration specific to certain behaviors, researchers were able to determine when each puma began its initial pursuit, the start of a high-speed chase, the moment of attempted

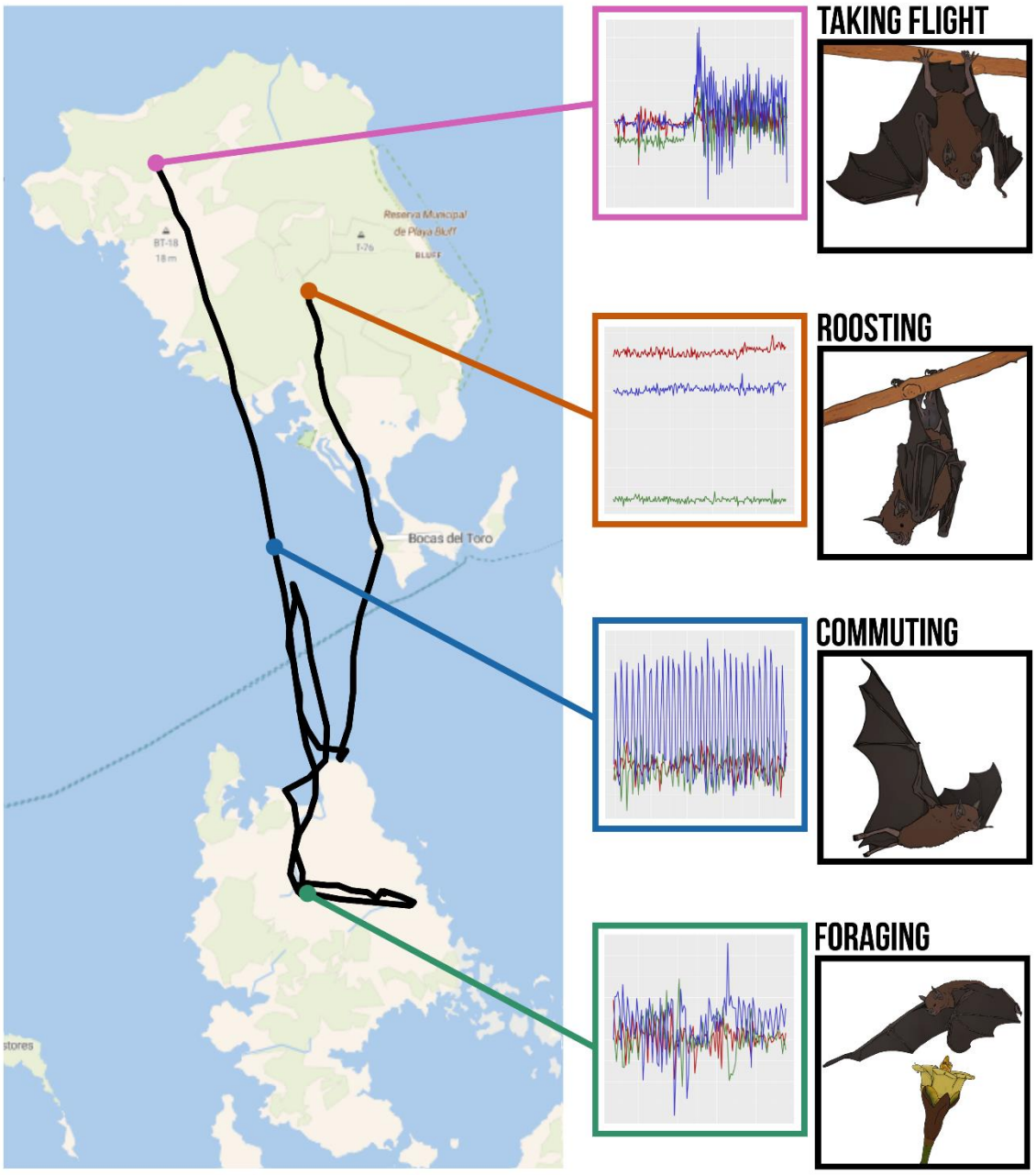

Figure 4. The movement path of a greater spear-nosed bat (GPS ID: Phyl38) during an entire night of foraging. The associated accelerometry data illustrates how unique changes in the bat's acceleration correspond to different behaviors performed throughout the night.

capture, and whether the hunt was successful. The data could even provide details about what *P. concolor* was hunting (e.g., buck or fawn) and was also used to estimate energy expenditure at each phase of the hunt. Changes in total power requirements were able to inform researchers about the amount of energy spent each hunt (Williams et al., 2014). This information can be used to create an estimation of the animal's energy requirements based on their movements, through calculating their total daily energy expenditure (DEE) (Barkse et al., 2014; Elliott et al., 2013; Green et al., 2009; Jeanniard-du-Dot et al., 2017a; Stothart et al., 2016).

Daily Energy Expenditure

Daily energy expenditure (DEE) serves as an estimate of the total amount of energy expended over a 24-hour period and represents a combination of the energy your body uses while at rest and your physical activity. Measures of dynamic body acceleration (e.g., VeDBA) can provide detail on a large portion of total DEE (Elliott et al., 2013; Jeanniard-du-Dot et al., 2017b; Jeanniard-du-Dot et al., 2017c; Stothart et al., 2016). This is especially true in animals where locomotion makes up a substantial portion of their energy expenditure (Bishop et al., 2015; Elliott, 2016; Elliott et al., 2013; Gleiss et al., 2011; Hicks et al., 2017; Stothart et al., 2016). Extended durations of DEE have been used to infer the impacts of anthropogenic pressures and the capability of an animal to adjust to declining habitat and resources (Castejón-Silvo et al., 2021; Green et al., 2009; Wang et al., 2017). Using DEE, we can also quantify the individual variability in

energy expenditure across social groups or populations, providing us with further context on dynamic foraging strategies and movement behaviors employed by certain animals (Barkse et al., 2014; Elliott et al., 2013; Jeanniard-du-Dot et al., 2017b; Jeanniard-du-Dot et al., 2017c; Stothart et al., 2016). Patterns in the spatial and temporal distribution of an animal's energy expenditure has been shown to be reflected in their DEE (Barkse et al., 2014; Elliott et al., 2013; Jeanniard-du-Dot et al., 2017b; Jeanniard-du-Dot et al., 2017c; O'Mara et al., 2023; Stothart et al., 2016), providing us with a way to quantify the success or efficiency of different foraging strategies or movement decisions (Barkse et al., 2014; Green et al., 2009; Weimerskirch, 2003).

Energy Landscapes and Modeling

Every organism has metabolic obligations that govern its day-to-day behaviors. An animal spends a large portion of its life obtaining the physical energy it requires from its environment to perform behaviors essential to life (Geiser, 2019; Houston and McNamara, 2014). These energetic demands, acquisition, allocation, and eventual expenditure encompass an energy landscape which reflects the spatial and temporal distribution of these energetic processes - known as an energy landscape (O'Mara et al., 2021; Scacco, 2021; Scacco et al., 2019; Shepard et al., 2013; Williams and Safi, 2021; Wilson et al., 2012).

Energy landscapes help shape our understanding of an animal's cost of movement, energy requirements, daily energy expenditure, and its general life history (Shepard et al., 2013). Animals modulate their movements as they

navigate their environment in a multitude of ways. They can alter their speed, chosen route, and the type, timing, frequency, and angle of movement (Dickinson et al., 2000). These movement decisions can be heavily influenced by dynamic environmental factors (i.e., resources, landscape, seasons, temperature, wind and weather conditions), and construction of energy landscapes provide a mechanistic approach to quantifying, determining and modeling decision-making and movement patterns of animals over time and space (Bishop et al., 2015; Masello et al., 2021; O'Mara et al., 2021; Shepard et al., 2013; Scacco, 2021; Scacco et al., 2019; Williams and Safi, 2021; Wilson et al., 2012).

When combined with predictive energy models, energy landscapes can provide clarification, and specific predictions of expected outcomes on individual to population level processes and movement decisions (Green et al., 2009; Klappstein et al., 2022; O'Mara et al., 2019). Quantifying and modeling an animal's distribution of energy over space and time provides an ecological link between the physical landscape, resource distribution, and movement choices (Scacco, 2021; Scacco et al., 2019; Shepard et al., 2013; Williams and Safi, 2021; Wilson et al., 2012). This approach also facilitates comparative studies across species or populations, improving our understanding of ecological strategies and responses to environmental changes (Shepard et al., 2013).

Species Background and Study Aims

Phyllostomus hastatus (greater spear-nosed bat) is an omnivorous bat that roosts in stable social groups consisting of unrelated females (Wilkinson et al.,

2016; McCracken and Bradbury, 1981). Greater spear-nosed bats are an extremely social species (McCracken and Bradbury, 1977, 1981) forming groups that can persist for as long as 16 years (Wilkinson and Boughman, 1998). The dynamic and strength of these social groups is thought to be the result of mutually beneficial behaviors such as cooperative foraging or the exchange of resource location information as well as mutual offspring protection and care (McCracken and Bradbury, 1981; Boughman, 2006).

A variety of bat species have been found to integrate social information about food into their foraging strategies using an assortment of cues (O'Mara et al., 2014; Page & Ryan, 2006; Ramakers et al., 2016; Ratcliffe & ter Hofstede, 2005; Wright, 2016). Greater spear-nosed bats have been shown to have the ability to identify group mates and communicate foraging information through group-specific vocalizations (Boughman & Wilkinson, 1998; Boughman, 1998; Wilkinson & Boughman, 1998; Wilkinson et al., 2016). A previous study has shown social proximity to have a positive influence on time *P. hastatus* spent outside of the roost and increased resting duration while out foraging (O'Mara & Dechmann, 2023).

Animals can be incentivized to participate in mutually beneficial behavior as it can increase foraging efficiency. Increased foraging efficiency can positively influence energy distribution through increasing the reliability of energy intake and decreasing the time and energy spent looking for food (Giraldeau and Beauchamp, 1999; McInnes et al., 2017; Snijders et al., 2021). These benefits

can be amplified when your food type is an ephemeral resource such as it is for the greater spear-nosed bat (O'Mara et al., 2014).

These bats live at their energetic ceiling, surviving on the energy provided by the day's feeding returns. To fulfill these energetic demands, *P. hastatus* alters their foraging strategies to match the seasonal changes and resulting resource shifts, switching between fruit (e.g., cecropia fruit) in the wet summer and the flower nectar (e.g., balsa flowers) in the dry winter, as well as insects and other small vertebrates (Wilkinson & Boughman, 1998). The dependence on ephemeral resources in the tropics can result in a larger diversity of foraging strategies, and consistent individual variation can stabilize cooperative behavior within populations (Bergmüller et al., 2010).

Populations with a higher degree of individual variation should be more likely to persist across a range of environmental conditions and adjust to changing resources (Caspi et al., 2022; Forsman and Wennersten, 2016). In *P. hastatus*, this can be seen in their variable route selection, foraging patch location, foraging strategy, and food choice (Boughman and Wilkinson, 1998; O'Mara and Dechmann, 2023; Wilkinson G. S. & Boughman, 1998). Changes in these movement-based decisions may result from the constantly shifting cost versus return of each foraging night. Adverse weather conditions can cause route changes, while poor food patch quality can prompt more exploratory foraging behavior. A decrease in food resources may lead to a dietary shift and changes in foraging locations. Conversely, consistent quality in any of these factors can lead to stable behaviors (Stephens and Krebs, 1986). These examples

demonstrate the numerous factors influencing how an animal allocates its energy expenditure over time and across its landscape.

In this study we aim to describe how accelerometry-based metrics of energy expenditure reflect measures of heart rate throughout a foraging night in the greater spear-nosed bat (*Phyllostomus hastatus*). Direct measurement of heart rate provides detailed insights into energy expenditure with high temporal resolution (Bishop and Spivey, 2013; Brown et al., 2022; Butler et al., 2004; Green, 2011; Green et al., 2008). By outfitting 11 greater spear-nosed bats with heart rate loggers and tri-axial accelerometers, we used heart rate to determine the quality of dynamic body acceleration (VeDBA) as an estimate of energy expenditure. Given that the cost of movement can be a substantial proportion of an animal's daily energy budget (King and Farner, 1961), we hypothesized that heart rate would positively reflect increases in VeDBA. Understanding that increasing and sustaining higher levels of activity requires increased energy costs, we also hypothesized that information on behavior would improve the accuracy of our energy estimates. Using these relationships, we also aim to construct movement-based energy landscapes detailing how individuals distribute their energy expenditure across time and space. By modeling and mapping the energetic framework of *P. hastatus*, we can provide context to their movement choices and associated costs. These calibrated energy landscapes allow for the exploration of how and why these bats make movement decisions, as well as provide more accurate estimates of their high-energy lifestyles.

CHAPTER II

METHODS

Study Overview & Design

All data used in this study were collected from 11 greater spear-nosed bats (*Phyllostomus hastatus*) that comprised one roosting group, consisting of 10 females and 1 harem male (**Table 1**). The roosting group was captured in a cave ('La Gruta') on Isla Colón, Bocas del Toro, Panamá using an elongated basket trap. Based on previous work of this species in Trinidad (Wilkinson & Boughman, 1998), roosting groups consisted of individuals co-roosting in small depressions in the cave's ceiling. All bats were caught as a group in one capture event and individuals were placed in breathable cotton draw-string bags and tied shut until being removed for processing.

The group was made up of 1 sub adult female, 1 adult male, and 10 adult females, with all being determined as non-reproductive. We recorded the mass of each bat to the nearest gram and measured their forearm length to the nearest 0.01 mm. Each bat was implanted with a passive integrated transponder (PIT) tag subcutaneously (Trovan ID -100, Euro ID, Weilerswist, Germany).

Table 1. Characteristics of greater spear-nosed bats tracked in this study. Information included is the weight, sex and relative age of the bat - noted as adult (A) or subadult (SA), forearm length, reproductive status - with all being non-reproductive (NR), GPS identification number (GPS ID), heart rate logger identification number (HRL ID), each bat's name within the data, and number of nights they were tracked.

Mass (g)	Sex	Age	Forearm (mm)	RS	GPS ID	HRL ID	Name	Nights
112	F	A	91.00	NR	Phyl32	1864UHL	Bia	5
118	F	A	93.20	NR	Phyl34	1863UHL	Aurora	5
110	F	A	89.43	NR	Phyl 30	1859UHL	Nyx	5
113	F	A	94.64	NR	Phyl 37	1855UHL	Athena	5
110	F	A	91.07	NR	Phyl 31	1857UHL	Artemis	5
111	F	A	92.05	NR	Phyl 38	1858UHL	Andromeda	4
117	F	A	93.45	NR	Phyl 36	1854UHL	Cassiopeia	5
128	F	A	90.55	NR	Phyl 35	1865UHL	Thalia	2
146	M	A	97.24	NR	Phyl 29	1861UHL	Ares	5
123	F	SA	93.30	NR	Phyl 33	1856UHL	Nike	5
126	F	A	93.20	NR	Phyl 40	1860UHL	Amphitrite	5
112	F	A	90.60	NR	Phyl 39	1862UHL	Pandora	3

Heart Rate & Body Temperature Logger Implantation and Removal

An integrated physiology logger (DST micro-HRT, 3 g, Star:Oddi, Gardabaer Iceland) was used to measure heart rate and body temperature from individual bats. Each logger was programmed to record heart rate at 600 Hz and body temperature every 60 s, with a full ECG recorded every 60 min. Each heart rate recording received a quality score (0-3, best - worst) based on the

manufacturer's scoring algorithm. Loggers were implanted subcutaneously on the dorsum of each bat under isoflurane anesthesia. Each animal experienced an anesthetic induction with 5% isoflurane delivered via a facemask (SomnoSuite, Kent Scientific Litchfield CT USA) and was maintained with 2% isoflurane and a heating pad was used to reduce the risk of hypothermia. A physical examination was performed, including lesions identification, body condition, hydration status, heart rate by auscultation, respiratory rate by visual detection, and rectal temperature by a commercial digital thermometer.

Exam found uniform and normal parameters among the 12 individuals. The middle and caudal dorsum were shaved and cleaned with antiseptic soap chlorhexidine 4%. The bats received a 0.2 mg/kg dose of meloxicam (OstiLox) and 8 ml/kg of fluids (NaCl) subcutaneously.

The surgical site was prepared with a 2% chlorhexidine scrub and isopropyl alcohol passages. A 1 cm horizontal skin incision was made with a surgical blade #15 in the middle-caudal dorsum. With a curved mayo scissor, the subcutaneous space was opened. The sterile logger was placed in the subcutaneous area, applying light pressure with the thumb and the index finger. The subcutaneous space was inspected for hemorrhage before closing and the skin was apposed anatomically and sutured with seven simple interrupted patterns using an absorbable suture (4-0 Coated Vicryl). Neomycin and clostebol spray (Neobol) were applied topically to the surgical wound site. The surgical procedure was consistent for all individuals and there were no complications present with the heart rate or respiratory rate. Temperatures dropped for the

majority of the animals after the surgeries. The animals were maintained in recovery bags until they were fully awake. The surgeries took 15 to 20 minutes on average. The whole procedure, with the presurgical preparation, took around 30 minutes. To remove the loggers, all bats underwent the same anesthesia procedure and exam. All animals presented a clean and healing surgical wound, and the loggers tended to be located laterally of the midline. No animal had loose sutures or signs of infection in the wound. The animals experienced the same presurgical preparation, induction, and maintenance as the first surgery. The bats received a 0.15 mg/kg dose of meloxicam (OstiLox), 10 ml/kg of fluids (NaCl) subcutaneously, and 5 mg/kg dose of enrofloxacin (Enroflox 10). For the surgical procedure, after the surgical site was prepared, an iris scissor was used to remove the skin sutures. The wound had a closed layer that was gently reopened using surgical blade #15. The logger was removed from the subcutaneous space by slight pressure and then the subcutaneous region was rinsed with saline. The free space in the subcutaneous was approximated with a simple interrupted suture. The edges of the skin wound were trimmed to revive the edges and allow the surgical closure. The skin was then apposed anatomically and sutured with seven simple interrupted patterns using an absorbable suture (4-0 Coated Vicrylt). Neomycin and clostebol spray (Neobol) were applied topically to the surgical wound site. The animals were maintained in recovery bags until they were fully awake and then released at the capture site.

GPS Logger Attachment

After recovery from surgery, all bats were outfitted with an epoxy-coated GPS and tri-axial accelerometer data logger (Axy-Trek Mini, TechnoSmart, Rome, Italy) that was attached to the dorsum caudally to the scapulae and cranially to the logger incision. The combined weight of the GPS and heart rate loggers was 7.8 g, ~6.6 ± 0.5% of mean ± SE body mass (range: 5.3-7.1%). The GPS tags were programmed to gather location data every one minute, between the hours of 18:00:00 to 05:00:00 local time (Eastern Standard Time). While actively tracking, a satellite search window of 2 minutes was set to obtain a GPS fix. During instances of poor reception, the GPS tags entered a low-energy sleep mode for 15 minutes before resuming a satellite search. Performance of each GPS tag varied due to the location of their roost (within a cave), their foraging sites being located in presumably dense forest, and resting under thick canopies. Tri-axial accelerometers were programmed to sample continuously at a frequency of 25 Hz at 10 bits with a dynamic range of ± 8g. Tags were positioned so the X-axis correlated to sway (left-right), Y-axis to surge (forward-backward), and Z-axis to heave (up-down).

Bats were recaptured using the same methods on the 6th day of deployment shortly after 06:00:00 (EST) and there was a 100% tag recovery rate for all loggers. We removed one bat from our analysis (GPS ID: Phyl30) as a result of inactivity and poor-quality data, providing us with data from 10 females and 1 male, with each bat tracked for 4.10 ± 1.16 nights (range:1.8-5 nights), for a total of 496.32 total tracking hours. Accelerometers and heart rate loggers

sampled continuously for the duration of the study and recorded 1,216.12 hours for each logging device. To estimate airspeed during flight, wind data were recorded at 15-minute intervals at an automated weather station (9°21’04”N, 82°15’29”W) managed by the Physical Monitoring Program at the Smithsonian Tropical Research Institute’s Bocas del Toro field station. Wind speed and direction measurements were taken every 10 seconds using an RM Young Wind Monitor Model 05103. At the end of each 15-minute interval, the mean wind speed and direction were calculated.

Data Analysis

Acceleration

All data were processed and analyzed in R version 4.2.2 (R Core Team, 2022), and summaries are presented as means ± SD.

To avoid unusual behavior caused by stress from the newly attached devices, the first night of data was also excluded from our data analyses. We calculated static acceleration, dynamic acceleration, vectorial dynamic body acceleration (VeDBA), and pitch from the raw tri-axial acceleration. Static acceleration (S_X, S_Y, S_Z) was calculated for each axis as:

$$S_{(X,Y,Z)} = \frac{\sum_X}{n}, \frac{\sum_Y}{n}, \frac{\sum_Z}{n} \quad \textbf{(1)}$$

Using the static acceleration, pitch (θ) was calculated as:

$$\theta = \tan^{-1}\left(\frac{S_X}{\sqrt{S_Y^2 + S_Z^2}}\right) * \frac{180}{\pi} \quad \textbf{(2)}$$

Dynamic acceleration (D_X, D_Y, D_Z) was calculated for each axis as total acceleration minus static acceleration:

$$D_{(X,Y,Z)} = S_X - X, S_Y - Y, S_Z - Z \quad \textbf{(3)}$$

and the Vectorial Dynamic Body Acceleration (VeDBA) was calculated as:

$$\mathrm{VeDBA} = \sqrt{A_X^2 + A_Y^2 + A_Z^2} \quad \textbf{(4)}$$

Each axis of acceleration (A_X, A_Y, A_Z) was summed, and we calculated a rolling average over a 2 second window to smooth the data for each acceleration metric. To bring the data to the same temporal resolution, estimates of VeDBA were summed to one minute to match the heart rate sampling rate.

Heart Rate

All raw heart rate data was first processed in Star:Oddi HRT Analyzer (Star:Oddi HRT Analyzer v.1.2.0. Mercury Application Software). Star:Oddi assigned Quality Index (QI) numbers ranging from 0 – 3 to each one-minute sample of data. 0 represents the highest quality data and 3 the lowest. Following manufacturer's recommendations, to remove any sampling errors from the data frame, a data quality check was done by removing all samples with a QI of 2 and 3, as recommended by Star::Oddi (Star:Oddi HRT Analyzer v.1.2.0. User Manual, August, 2023). Based on minimum and maximum heart rates for *P. hastatus* from

previous literature (Thomas & Suthers, 1972), we removed heart rates above 900 beats per min^{-1} and below 100 beats min^{-1}. Together, these corrections resulted in a ~22% loss of our data. We observed no bias towards high or low values in the heart rate quality index. Each night of every bat's heart rate data was joined with the corresponding accelerometry data by timestamps. We estimated energy expenditure from heart rate data (Bishop & Spivey, 2013) by modeling oxygen consumption as a function of heart beat frequency (f_H), heart mass (M_h) and body mass (M_b) (**Eq. 5**).

$$\dot{V}O_2 = 0.0402 \times M_b^{0.328} \times M_h^{0.913} \times f_h^{2.065} \quad \textbf{(5)}$$

We estimated *P. hastatus'* heart mass to be ~1% of its total body mass (Canals et al., 2005, Thomas & Suthers, 1972). $\dot{V}O_2$ was then converted to joules per minute (1 ml O_2 = 21.11 J; $\dot{V}O_2$ * 21.11) (O'Mara et al., 2017), and finally to kilojoules per minute.

Behavior Classification

Acceleration data were manually inspected to section out durations of known behaviors using a basic understanding of flight physics and visual inspections of plotted data (**Figure 5**). Distributions of metrics from identified behavior (flying, roosting, crawling/scratching) provided the minimum, maximum, and most meaningful values for each variable during each behavior.

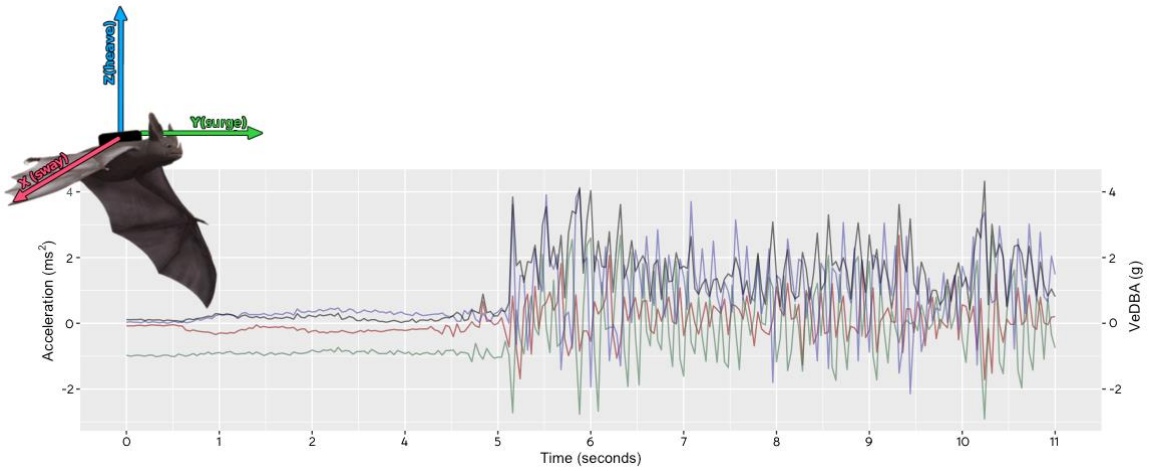

Figure 5. Raw tri-axial acceleration data plotted with values of VeDBA (black line) estimated from it. The data is derived from 10 seconds of tri-axial accelerometry data from the moment a greater spear-nosed bat takes off for flight, showing the significant changes seen in acceleration from each axis, and the values of VeDBA reflected by it. Tri-axial accelerometers record acceleration in all three axes as shown by the bat in the upper corner of the figure. The X axis (sway) is represented by red, the Y axis (surge) by green, and the Z axis (heave) by blue.

Metrics with clear and useful differences between each behavior were then selected for our decision tree (**Figure 6**). A threshold towards the floor or ceiling of each behavior distribution, whichever was more likely, was chosen for the breakpoints in the tree. Depending on the quality of the threshold at identifying the unique behavior, flight metrics were hierarchically arranged in the tree. To smooth out potential errors in the behavioral classification model, behaviors occurring for less than one second were assigned to the previous behavior.

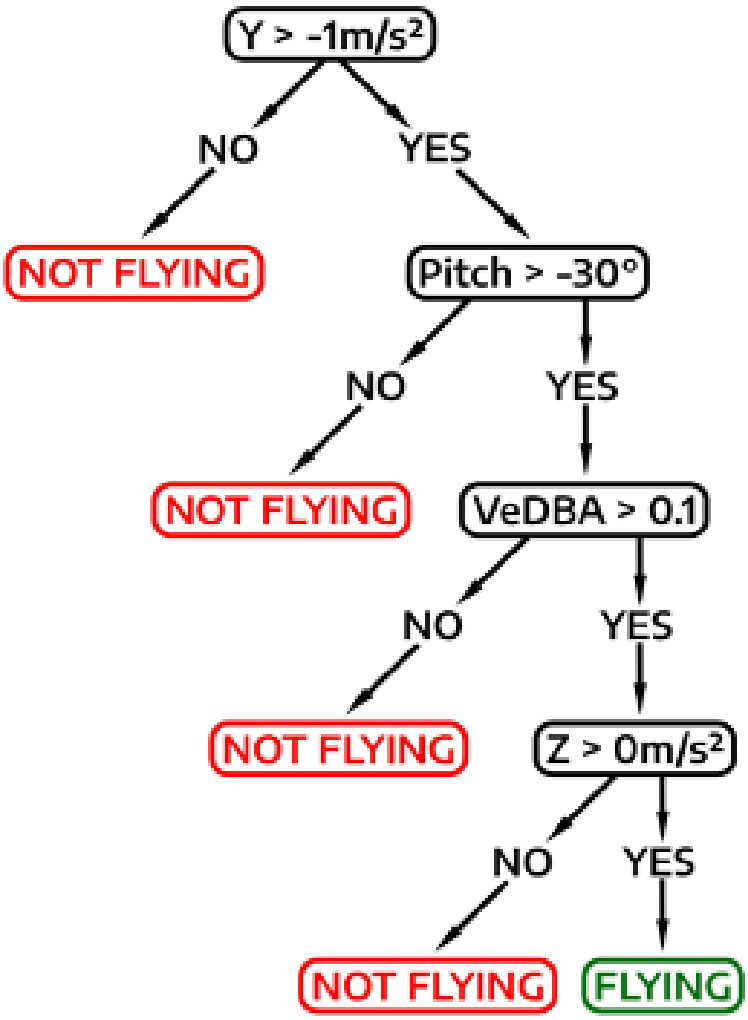

Figure 6. Behavioral decision tree showing the thresholds and classification hierarchy used to classify occurrences of flight for Greater spear-nosed bats. Decisions are ranked by their significance in identifying the behavior, with most significant at the top.

Flight sequences were further categorized into commuting flight when applicable. Commuting flight was defined as any duration of flight lasting longer than 3 minutes and excluded the first and last 30 seconds of a flight sequence to account for landing and take-offs.

Modeling

Heart rate should reflect a high fidelity estimate of energy expenditure (Bishop & Spivey, 2013; Thomas & Suthers, 1972). To determine possible relationships between heart rate and other estimates of energy expenditure, including VeDBA and airspeed, we constructed generalized additive mixed effect models (GAMMs). The rate at which our energy expenditure metrics change can vary between variables, depending on different behaviors, environmental conditions, and kinematic adjustments and the use of GAMMs allows for more appropriate modeling of energy expenditures that do not follow normal distributions. Tag ID was included as a random effect in all of our models. The structure of our baseline model was that heart rate was predicted by VeDBA or airspeed (e.g., *heart rate ~ VeDBA)*. This was used to determine any initial relationship between each metric and serve as a "type model" to compare our following models to. Since the maximum rate of oxygen consumption works as an asymptote (Bishop & Spivey, 2013), we wanted to understand how this model would respond to an estimate of energy expenditure derived from our heart rate data (kJ min^{-1}) as our dependent variable, instead of the heart rate data itself (Hicks et al., 2017). We structured this model as *energy expenditure ~ VeDBA*.

Sustaining increased physical activity requires a continual supply of oxygen pumped to the working muscles, which would be reflected in an individual's elevated heart rate. We incorporated the effect of behavior (not flying, flying) into our models to understand how changes in heart rate reflects changes in VeDBA across two different levels of activity. We included the interaction

between the behavior being performed and VeDBA using *heart rate ~ (VeDBA):activity*. This was also completed for our models containing the heart rate-derived estimate of energy expenditure (kJ min^{-1}).

We used a multi-inference approach to select the best fitting models to describe the relationship between heart rate (or energy expenditure) and subsequent predictors. The p-value of each independent variable included in every model was calculated to determine the significance of its effect on the model's outcome. The t-value was calculated to show the magnitude of the estimated effect on the dependent variable in each model. Models with larger t-values suggested greater confidence in the significance of the estimate. The standard error of each model's dependent variable values was calculated. Small standard errors provided us with more information on which models had more reliable estimates. The Effective Degrees of Freedom (edf) were calculated for each predictor variable (also known as smooth terms within the model). The edf reflects the complexity of the smooth terms in the model, and models with higher edf are more complex, with edf of 1 reflecting a straight linear fit. The adjusted R-squared (R^2 (adj)) of each model was calculated to measure how well the model explained the variability of the dependent variable. As more smoothed terms were added and the complexity of our models increased, the R^2 (adj) was penalized. Finally, we used the Akaike Information Criterion (AIC) to evaluate the goodness-of-fit between models with the same dependent variables. The AIC balances the trade-off between model complexity and goodness-of-fit. Our

models with lower AIC values indicate a better fit, and we considered all models within two AIC units of the best fit models as equally likely.

Ethical Statement

This study was approved by the Ministerio del Ambiente, Panamá (SE/A-38-2020) as well as the Animal Care and Use Committee at the Smithsonian Tropical Research (SI-23016-1) and to the ASAB/ABS Guidelines for the Use of Animals in Research.

CHAPTER III

RESULTS

Behavior and Tracking Summary

Bats emerged from the roost at 20:50:35 ± 1.16 hours (Eastern Standard Time mean ± SD). The bats returned to their roost at 05:23:00 ± 1.86 hours. This results in a total of 47.78 hours of GPS data, 1,512 hours of accelerometry data, and 1,512 hours of heart rate data. We identified 18 foraging/resting sites from 8 individuals. These bats traveled an average distance of 17.73 ± 4.14 km to reach off-island foraging/resting sites, with an average of 5.96 ± 2.05 km of that commute flown over the ocean.

Bats began their commute with slight head winds and returned to their roosts with slight tailwinds. Wind was generally low and variable in speed and direction throughout each foraging night, with an average wind speed of 9.5 ± 7.44 ms^{-1}. Notably, on the second night of tracking, wind speed peaked at 21.98 ms^{-1} at the time of emergence.

Bats primarily divided their time between two aggregations of over-ocean foraging sites, (**Figure 7**). Clustered foraging sites were located off of the island they roosted on and reaching them entailed crossing a significant stretch of ocean (2-10 km). One over-ocean grouped foraging site was located on the mainland roughly 2 km southeast from the city of Changuinola (**Figure 7 - Site 1**), and the other was located on Isla Cristóbal (**Figure 7 - Site 2**), an island directly south from the city of Bocas del Toro. The third foraging location was in

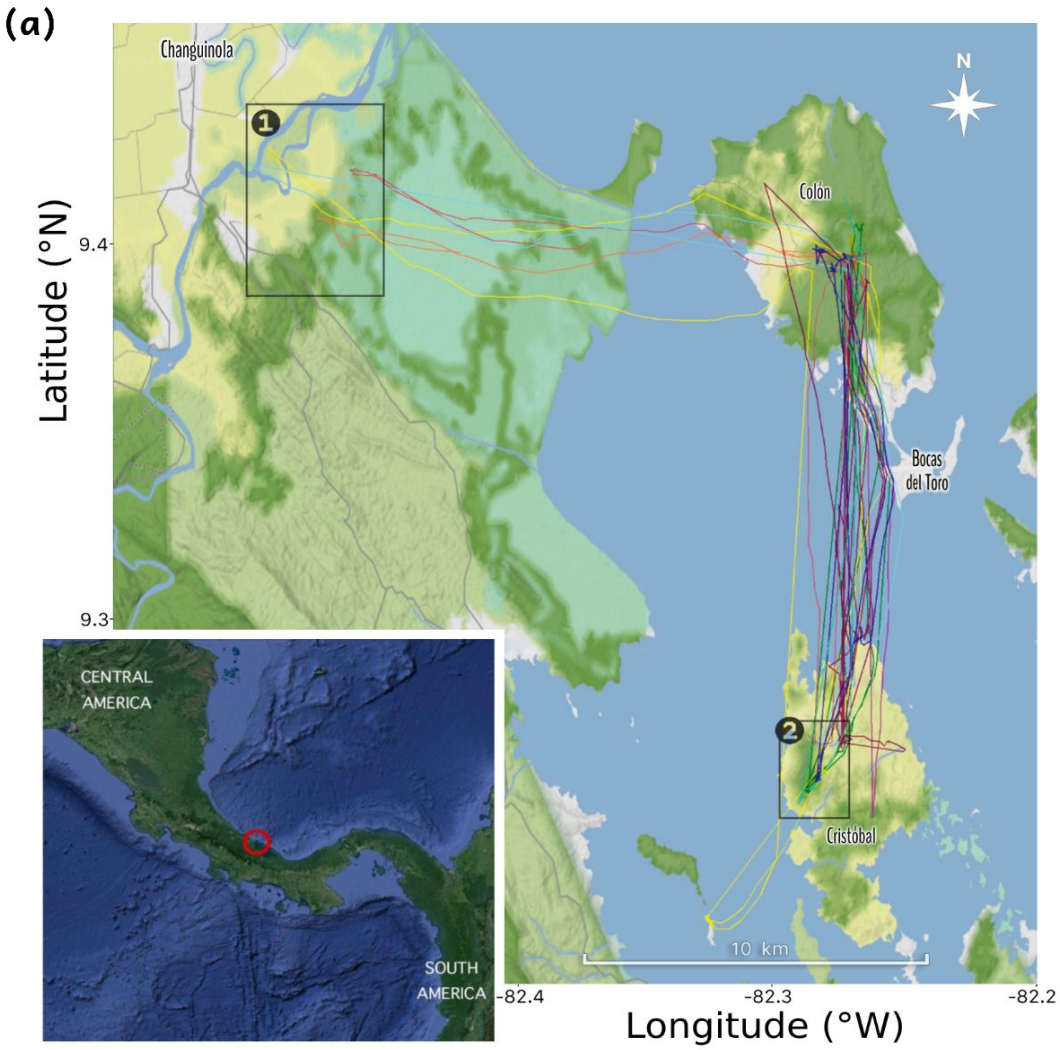
(a)
Changuinola
1
N
Colón
Bocas
del Toro
2
Cristóbal
10 km
CENTRAL
AMERICA
SOUTH
AMERICA
Latitude (°N)
9.4
9.3
-82.4
-82.3
-82.2
Longitude (°W)

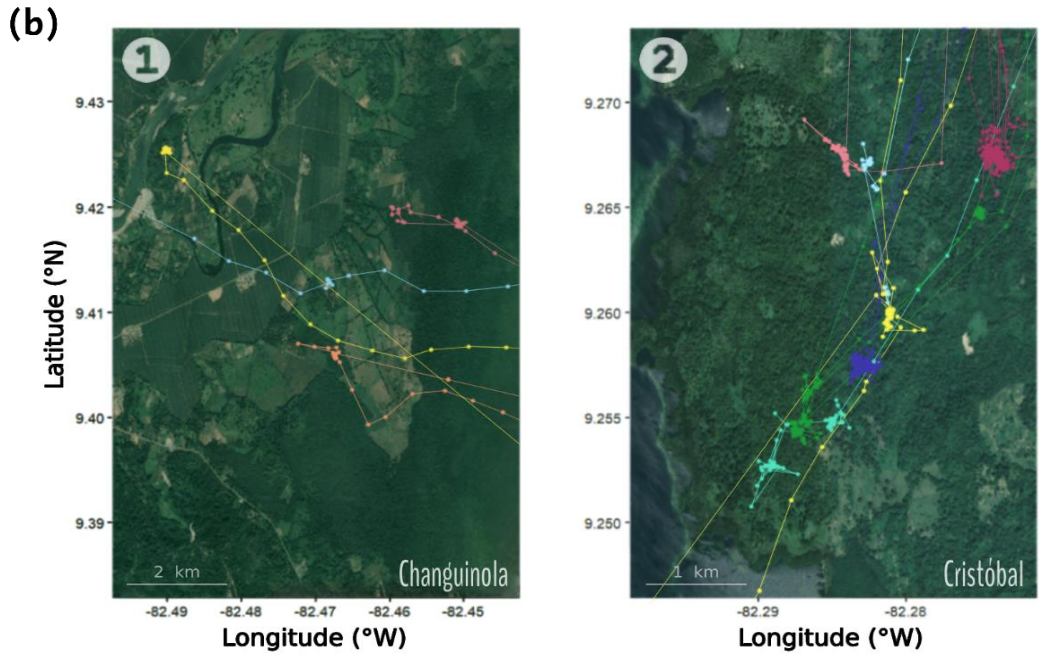
(b)
1
9.43
9.42
9.41
9.40
9.39
Latitude (°N)
2 km
Changuinola
-82.49
-82.48
-82.47
-82.46
-82.45
Longitude (°W)
2
9.270
9.265
9.260
9.255
9.250
1 km
Cristóbal
-82.29
-82.28
Longitude (°W)

Figure 7 (a) - Tracked routes across 6 nights show foraging behavior, colored by individual bats. Numbered black boxes indicate two main foraging aggregations. The outset shows the isthmus connecting North and South America, with Isla Colón marked by a red circle. **(b)** Numbered insets zoom in on the two primary foraging aggregations, detailing each foraging cluster's location.

the nearby forest surrounding their roost on Isla Colón. During this study, bats were more likely to visit Isla Cristóbal (Site 2, 19 of 24 trips) which was 11-16 km away from their roost, than Changuinola (Site 1, 5 of 24 trips) which was 20-25 km away from the roost.

One individual (**Table 1 - Aurora**) was recorded making additional stops to foraging sites on a small island southwest of Cristóbal (Site 3) after foraging there. The foraging sites on this island (Isla Pastores) were an additional 6.5 km away from their previously visited foraging sites on Isla Cristóbal (Site 3). This individual was observed returning to the same two sites, each on different islands, within consecutive nights. While no individuals were observed visiting the same patch of trees as another individual, not even on separate nights, individuals did seem to distribute their foraging sites within a relatively close proximity from each other's (described by the foraging aggregations), although not always visiting the same aggregations as each other on the same night.

Energy Expenditure Across Time

The energy expenditure of *Phyllostomus hastatus* was primarily distributed between the local sunset and sunrise, shown by the shaded region in **Figure 8c**. During night hours, the average heart rate of *P. hastatus* was 254.13 ± 94.24 beats min^{-1} (range: 101-800 beats min^{-1}). The average nightly VeDBA was

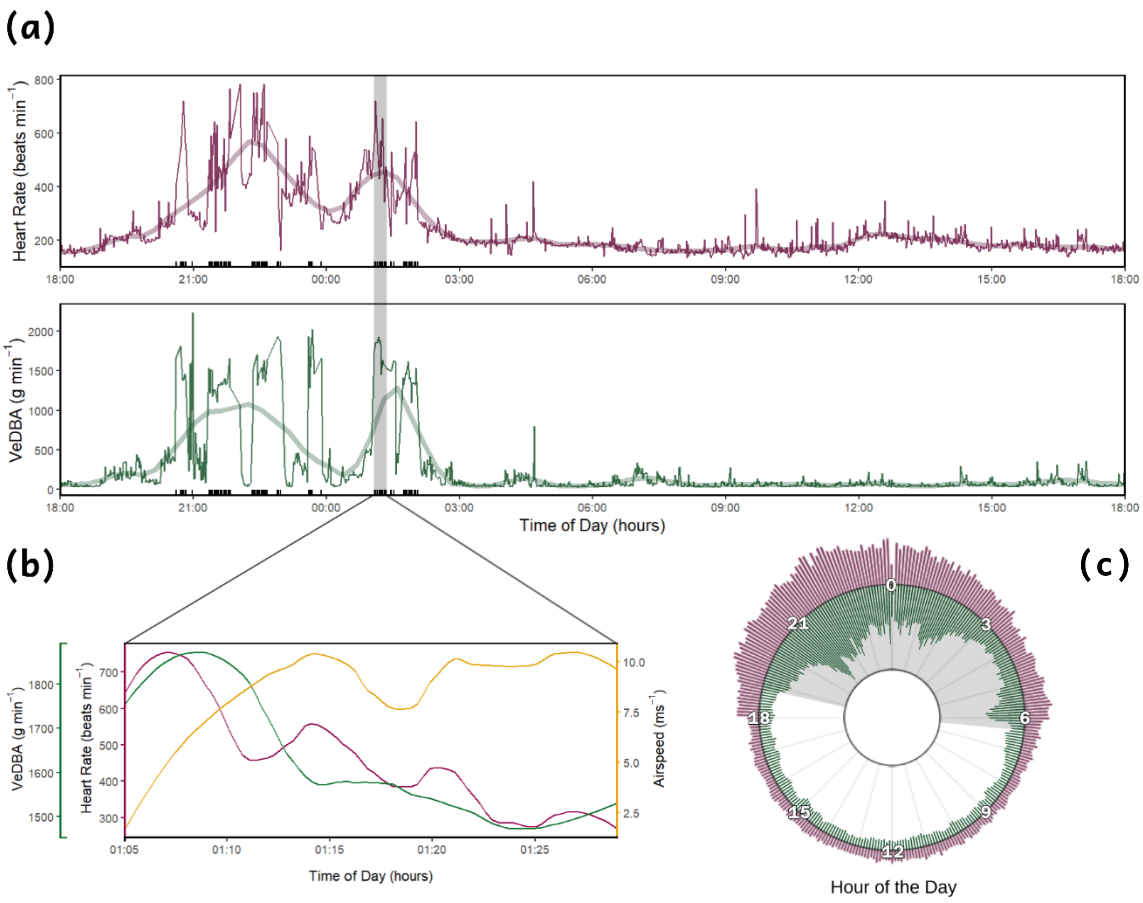

Figure 8. Comparisons between energy metrics illustrating the temporal distribution of energy expenditure in various contexts. **(a)** Shows heart rate [violet] and VeDBA [green] data across a 24-hour period for bat GPS ID: Phyl38. Black bars below each plot represents times of identified flight. **(b)** Inset zooms into 25 seconds of flight metrics from (a) (duration represented by grey vertical band), comparing changes in heart rate and VeDBA to airspeed [yellow]. **(c)** Presents a 24-hour clock depicting average heart rate and VeDBA distribution by time of day, with shaded regions indicating the period between local sunset and sunrise.

295.08 ± 441.57 g min^{-1} (range: 23.61-3,023.74 g min^{-1}). During the day (06:00:00 - 18:00:00 EST), the average heart rate was 194.09 ± 58.41 beats min^{-1} (range: 101-800 beats min^{-1}). The average daily VeDBA was 105.44 ± 100.03 g min^{-1} (range: 22.45-2,064.59 g min^{-1}). As airspeed increased, our energy metrics (heart rate, VeDBA) gradually decreased (**Figure 8b**). Once emerged from their roost, bats spent an average of 74.82 ± 44.01 minutes

flying/foraging, and 297.40 ± 145.97 minutes resting. After sunset (18:50:00 EST), Activity peaked during the hours of ~21:00:00, ~01:00:00, and ~05:00:00 (EST), with an average heart rate of 272.95 ± 46.92 beats min^{-1}, and average VeDBA of 403.62 ± 146.65 g min^{-1} during these hours (**Figure 8c**). Throughout the night, activity was the lowest at ~04:00:00 (EST), with an average heart rate of 208.88 beats min^{-1}, and average VeDBA of 134.65 g min^{-1} during this hour.

Energy Expenditure Across Activity

When analyzing how each metric of energy expenditure was distributed during different levels of activity, there was multiple similarities shared between heart rate and VeDBA observed.

Vectorial Dynamic Body Acceleration

During rest, VeDBA was characterized by a condensed aggregation of low values with a mean VeDBA of 130.66 ± 135.18 g min^{-1}, yet had a large range of 22.45-2,565.91 g min^{-1}. Likely due to short bouts of energetically intensive behavior such as crawling depicted in the thin green horizontal line extending from the right of the VeDBA's distribution in **Figure 9 (Rest)**. While flying, VeDBA was considerably higher than during rest for greater spear-nosed bats (**Figure 9**, p-value < 0.001).

Flight was characterized by a wider distribution of higher values with average VeDBA of 1,426.52 ± 366.46 g min^{-1}, and ranged from 127.20-3,023.74

g min^{-1} across all types of flight (take off, commuting, foraging, and landing) (**Figure 9 - VeDBA | Rest** - mean: 87.47, σ^2: 18273.71, Q1: 50.76, Q3: 162.73; **Flight** - mean: 1377.57, σ^2: 134293, Q1: 1192.22, Q3: 1666.04). VeDBA experienced a 991.4% increase during flight.

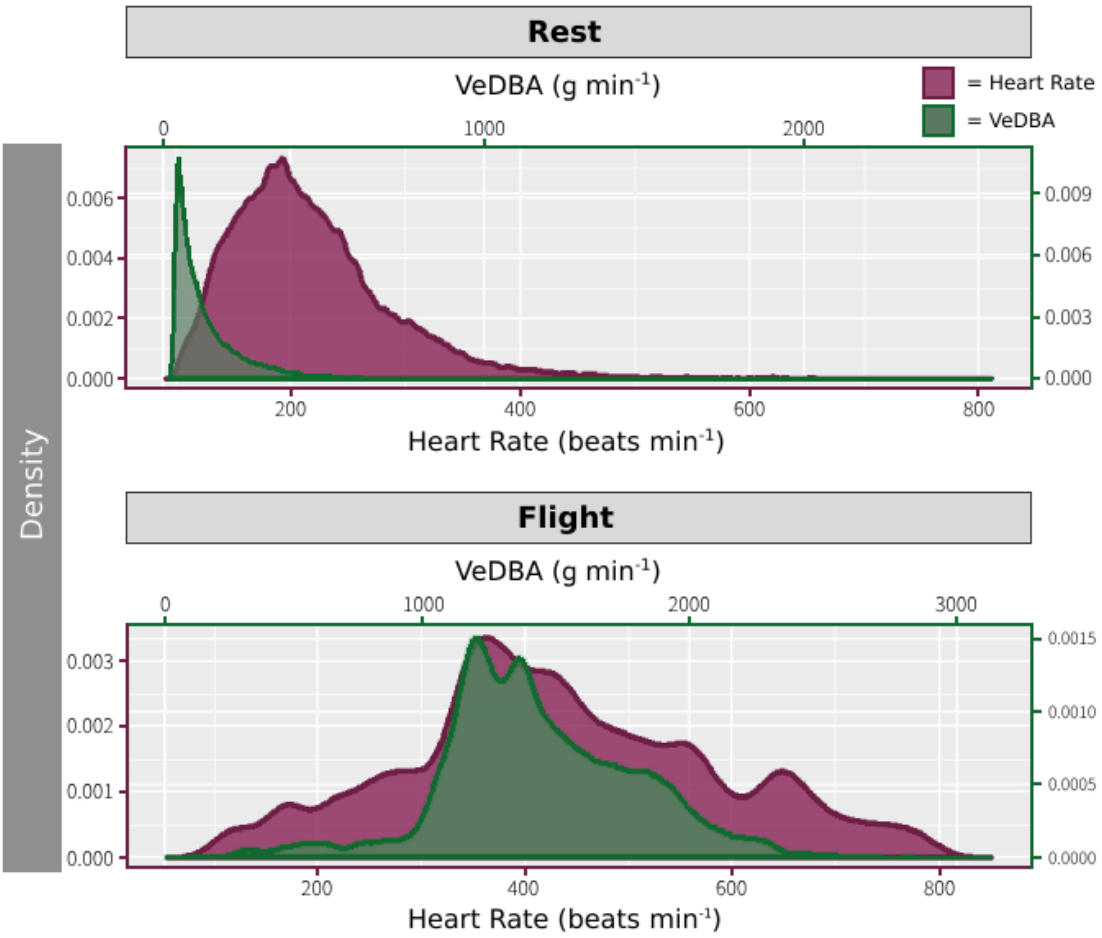

Figure 9. Density plots illustrating the distribution of heart rate and VeDBA data during periods of rest and flight among bats. Heart rate and its respective scales are indicated by the violet coloration. VeDBA and its scales are indicated by the green coloration. During times of rest, energy metrics become aggregated at low levels, while during flight, the metrics become more widely distributed at higher values.

Heart Rate

The same contrasting distribution observed in VeDBA between high and low activity levels was also observed in the distribution of heart rate (**Figure 9**).

Similar to VeDBA, heart rate at rest was primarily distributed towards the lower plot values. Although, heart rate during rest exhibited a larger distribution than that of VeDBA during rest, with a range of 101-800 beats min^{-1} and average resting heart rate of 218.95 ± 75.51 beats min^{-1}. During flight, bats had an average heart rate of 434.21 ± 149.92 beats min^{-1} (range: 105-800 beats min^{-1}). Heart rate showed a broader distribution during flight, with an increased frequency at higher rates across the scale (**Figure 9 - Heart Rate | Rest** - mean: 205, σ^2: 5701.28, Q1: 168, Q3: 251; **Flight** - mean: 418, σ^2: 22474.80, Q1: 342, Q3: 418). Heart rate experienced a 98.3% increase during flight.

Airspeed

To understand how airspeed interacted with energy expenditure and whether we would observe a similar power curve in field-collected data from *P. hastatus*, we initially examined the distribution of all three of energy metrics during flight (**Figure 10**). Across all types of flight, we saw airspeed primarily distributed at higher and lower airspeeds, with a majority of the distribution above 6 ms^{-1} (**Figure 10 | Airspeed** - mean: 7.46, σ^2: 13.53, Q1: 2.16, Q3: 9.28). Airspeeds below 3 ms^{-1} accounted for ~31.53% of all flight speed data.

Of these low airspeeds, the first and last 60 seconds of a flight duration, and flights lasting less than 60 seconds accounted for 78% of these data, so it is likely that most of these low flight speeds consist of short flights, take-offs, and landings. Airspeeds between 3-6 ms^{-1} accounted for only ~10.72% of our flight speed data. *P. hastatus* spent very little time flying at median airspeeds. The

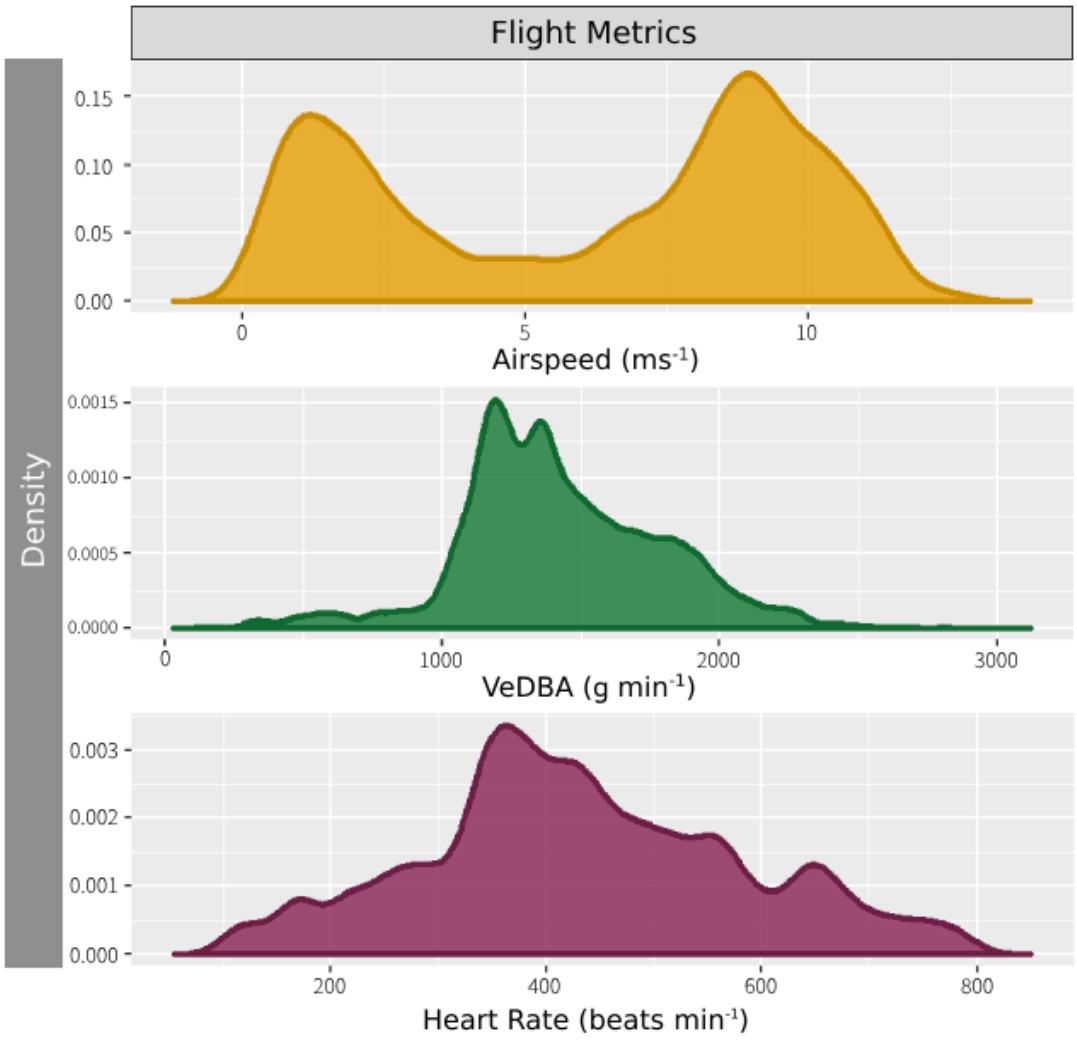

Figure 10. Density plots illustrating the distribution of airspeed, heart rate and VeDBA data during periods of flight among bats. Additionally, airspeed is indicated by the yellow coloration.

majority of time spent flying was at airspeeds above 6 ms^{-1}, which made up ~57.76% of the flight speed data. Throughout all foraging nights, greater spear-nosed bats flew at airspeeds ranging from 0.08-12.59 ms^{-1}, resulting in an average airspeed of 6.15 ± 3.68 ms-1 across all types of flight. This was similar to minimum power speeds (6.81 ± 0.21 ms-1) from average power curves estimated for P. hastatus (O'Mara & Dechmann, 2023). Additionally, ~48.68% of

all airspeeds were flown between their estimated minimum power speed (6.81 ± 0.21 ms-1) and maximum range speed (11.0 ± 0.35 ms-1). This range of airspeed is estimated to be the least energetically costly to fly at for greater spear-nosed bats (O'Mara & Dechmann, 2023).

Estimating Energy Expenditure from Heart Rate

During rest, bats expended an average of 0.07 ± 0.06 kJ min^{-1}, with a range of 0.01-0.96 kJ min^{-1}. In comparison, while flying, an average of 0.28 ± 0.18 kJ min^{-1} was expended, and ranged from 0.01-1.08 kJ min^{-1} across all types of flight (**Table 2**). The average estimated daily energy expenditure was 143.29 ± 30.18 kJ day^{-1} (range: 101.43-209.71 kJ day^{-1}) (**Figure 11**). These estimates are similar to previous ones from the same species captured in the same cave of 198.47 ± 69.44 kJ day^{-1} (O'Mara & Dechmann, 2023) as well as estimates using only body mass of 153.02 ± 5.96 kJ day^{-1} (range: 143.07-164.89 kJ day^{-1}; Speakman, 2005).

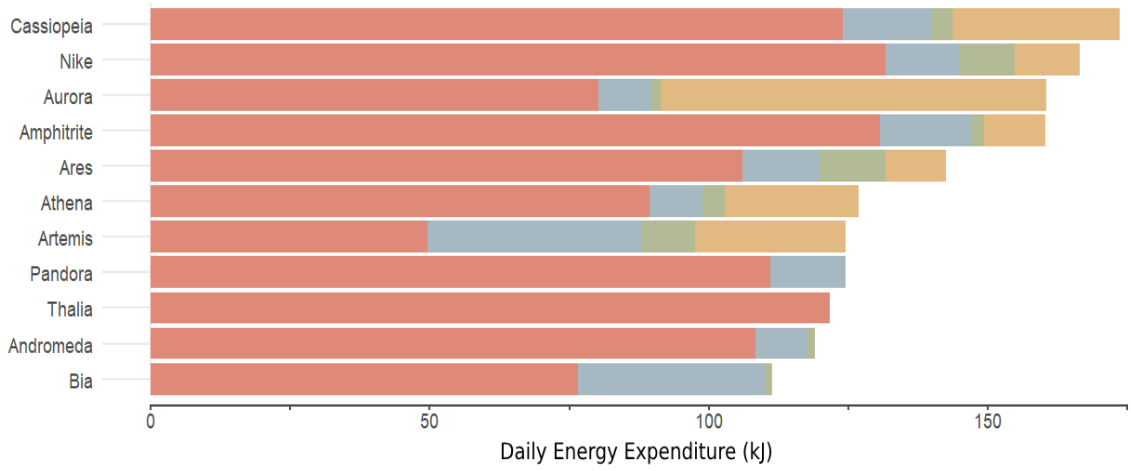

Figure 11. Daily energy expenditures (DEE) for each individual bat. Change in color within each bar represents a different day with a higher DEE than the previous day.

Table 2. Energy expenditure and morphological data of individual bats. Information includes sex, body weight (M_b), heart weight (M_h), average rate of oxygen consumption during flight ($\bar{X}$ $\dot{V}O_{2\,F}$), average energy expenditure during flight ($\bar{X}$ $VeDBA_F$), name of bat within data set, and heart rate logger ID.

Sex	M_b (kg)	M_h (kg)	$\bar{X}$ $\dot{V}O_{2\,F}$ (ml min^{-1})	$\bar{X}$ EE_F (kJ min^{-1})	$\bar{X}$ $VeDBA_F$ (g min^{-1})	Name	HRL ID
F	0.112	0.00110	16.22	0.342	1479.13	Bia	1864UHL
F	0.111	0.00109	12.26	0.259	1572.64	Andromeda	1858UHL
M	0.146	0.00143	12.12	0.256	1640.57	Ares	1861UHL
F	0.112	0.00110	10.67	0.225	1422.22	Pandora	1862UHL
F	0.118	0.00116	9.93	0.210	1395.72	Aurora	1863UHL
F	0.113	0.00111	9.80	0.207	1343.01	Athena	1855UHL
F	0.117	0.00115	8.58	0.181	1263.79	Cassiopeia	1854UHL
F	0.128	0.00125	8.43	0.178	1274.95	Thalia	1865UHL
F	0.123	0.00121	8.40	0.177	1384.44	Nike	1856UHL
F	0.110	0.00108	8.27	0.175	1309.22	Artemis	1857UHL
F	0.126	0.00123	6.04	0.128	1292.59	Amphitrite	1860UHL

Modeling Energy Expenditure

Each model incorporated a different combination of energy metrics and behavioral interactions aimed at finding the model that best represents the true nature of the relationship between heart rate and the various estimates of energy expenditure. Model results, including how each was structured, their statistics, and relative performance values are included in **Table 3**.

VeDBA & Heart Rate Relationship

Our first model (**Figure 12 | Model 1**), compared only heart rate and VeDBA. We found a positive dynamic relationship (p-value < 0.001, t = 36.01) between heart rate and VeDBA.

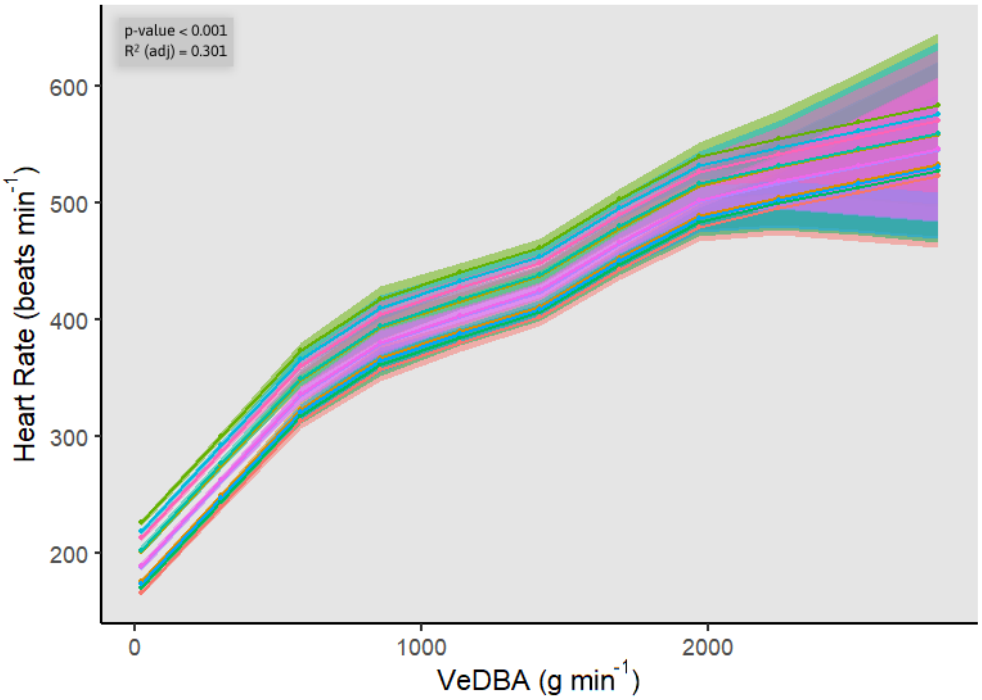

Figure 12 | Model 1. The relationship of VeDBA and heart rate. Each color represents the GAMM results for a different individual. The p-value and R^2 (adj) are shown in the upper corner for each model.

Using VeDBA as the only smooth effect when predicting heart rate provided an edf of 8.459. Overall, the model received an AIC score of 508,410.80. Our model shows that in general, when a bat increased its dynamic body acceleration (VeDBA), this was positively correlated with an increase in the frequency of each heart beat.

To better understand how the relationship between heart rate and VeDBA may change between different behaviors, we modeled the predictability of VeDBA for heart rate for periods of rest and times of flight (**Figure 13 | Model 2**). We incorporated the interaction between VeDBA and the behavior being performed (not flying, flying), which allowed us to determine if the value of VeDBA as a predictor of energy expenditure is dynamic between levels of

activity. VeDBA predicted heart rate across all model types (**Figure 12 & 13,** p-value < 0.001). However, the best fit model for predicting heart rate from VeDBA included behavior state (**Table 3**).

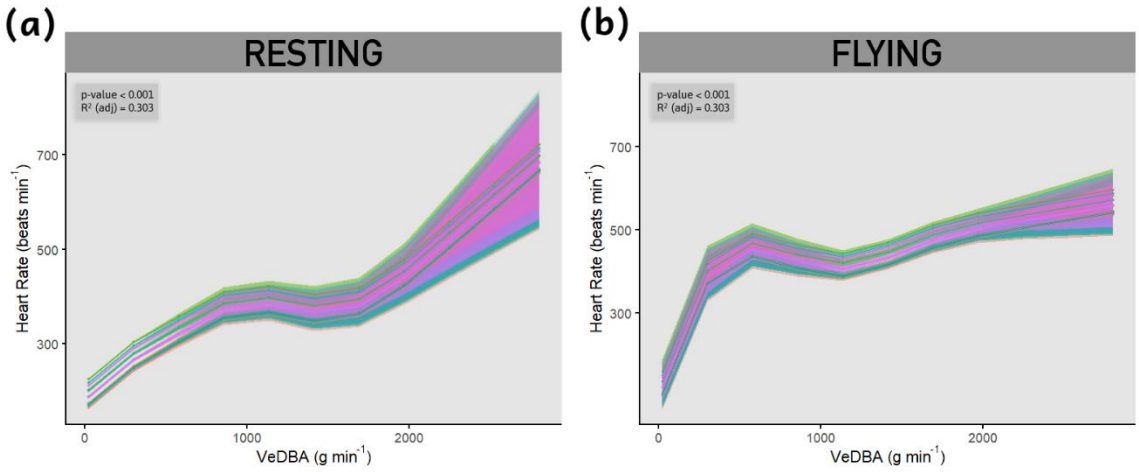

Figure 13 | Model 2. Heart rate during rest **(a)** and during flight **(b)** relative to VeDBA. Each color represents the GAMM results for a different individual. The p-value and R^2 (adj) are shown in the upper corner for each model.

By separating these data based on behavior (**Model 2**), we observed a statistical improvement across all tests from our baseline model (**Model 1**). When behaviorally classified, VeDBA performed slightly better at explaining change in heart rate with greater confidence (**Model 1** - R^2 (adj): 0.301, t = 36.01; **Model 2** - R^2 (adj): 0.303, t = 36.06). These values of heart rate were also estimated with a smaller degree of error (**Model 1** - 225.350 ± 6.258; **Model 2** - 224.28 ± 6.22). We concluded that informing our models on which behavior the bat is performing provides a better fit than our simpler model and improves the model's accuracy and explanatory power for heart rate (**Model 1** - AIC: 508,410.8; **Model 2** - AIC: 508,289.3).

While we increased the complexity of the model as a whole, by classifying behavior, the complexity of the relationship between VeDBA and heart rate decreased, likely representing a more parsimonious nature of the relationship (**Model 1** - edf: 8.459; **Model 2** - edf: 4.596, 4.885). Model results of flight showed a substantial spike in heart rate during the initial increase in VeDBA, followed by a brief decline before slowly increasing.

To establish an initial relationship between VeDBA and $\dot{V}O_2$, we used our estimates of energy expenditure (kJ min^{-1}) derived from our $\dot{V}O_2$ values. We structured the model as *energy expenditure ~ VeDBA*. A positive relationship was also observed between heart rate-derived energy expenditure (kJ min^{-1}) and VeDBA (**Figure 14 | Model 3**) (p-value < 0.001). Our analyses showed higher degree of confidence in the significance of the estimate (**Model 1** - R^2 (adj): 0.301, t = 36.01; **Model 3** - R^2 (adj): 0.286, t = 17.81). **Model 1** better explained the variability of the dependent variable and had a higher degree of confidence in the significance of the estimate (**Model 1** - R^2 (adj): 0.301, t = 36.01; **Model 3** - R^2 (adj): 0.286, t = 17.81). When using VeDBA to predict energy expenditure (kJ min^{-1}), the complexity of VeDBA's relationship with the dependent variable increased (**Model 1** - edf: 8.459; **Model 3** - edf: 8.582), and the standard error also made up a larger percentage of the dependent variable's values (**Model 1** - 225.350 ± 6.258; **Model 3** - 0.074742 ± 0.004196). **Model 3** received an AIC of -123,146.5.

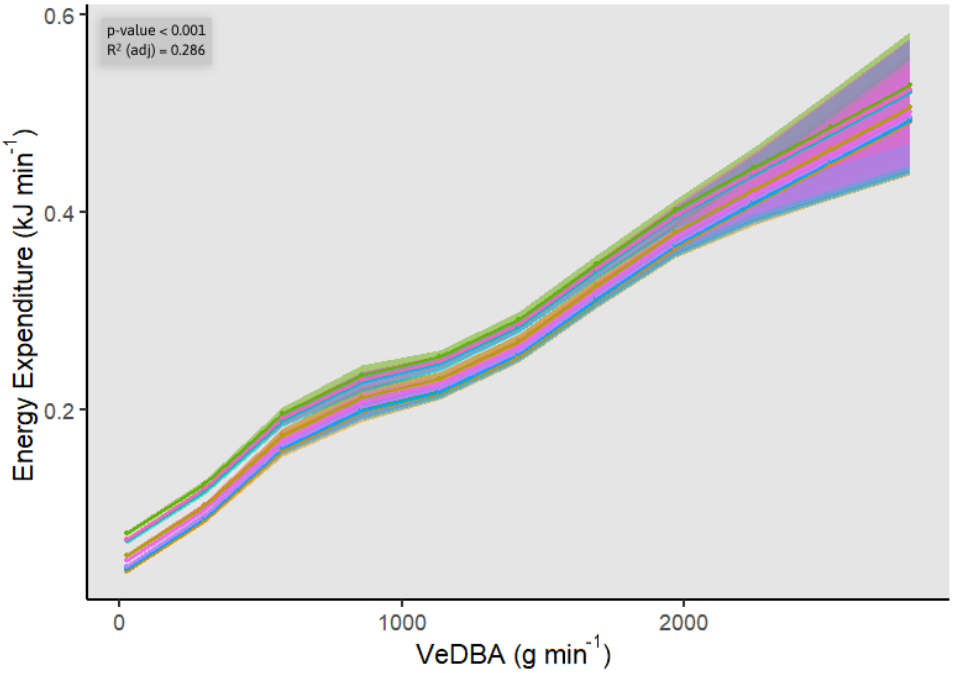

Figure 14 | Model 3. The relationship of VeDBA and energy expenditure (kJ min^{-1}). Each color represents the GAMM results for a different individual. The p-value and R^2 (adj) are shown in the upper corner for each model.

We wanted to understand if different levels of activity also resulted in changes to the relationship between oxygen consumption ($\dot{V}O_2$) and accelerometry, so models predicting energy expenditure (kJ min^{-1}) were also behaviorally classified. Just as we observed in the comparisons of **Model 1 & 2**, complexity of VeDBA's relationship with the dependent variable decreased when behaviorally classified (**Model 3** - edf: 8.582; **Model 4** - edf: 4.690, 4.895). We also saw an increase in reliability in our model's estimates of energy expenditure (kJ min^{-1}) using behavioral classification (**Model 3** - AIC: -123,146.5, R^2 (adj): 0.286; **Model 4** - AIC: -123,383.5, R^2 (adj): 0.290). Similar differences in the relationship between VeDBA and heart rate observed during resting and flying (**Model 2**) were also seen in VeDBA's relationship with energy expenditure (kJ min^{-1}) across behaviors.

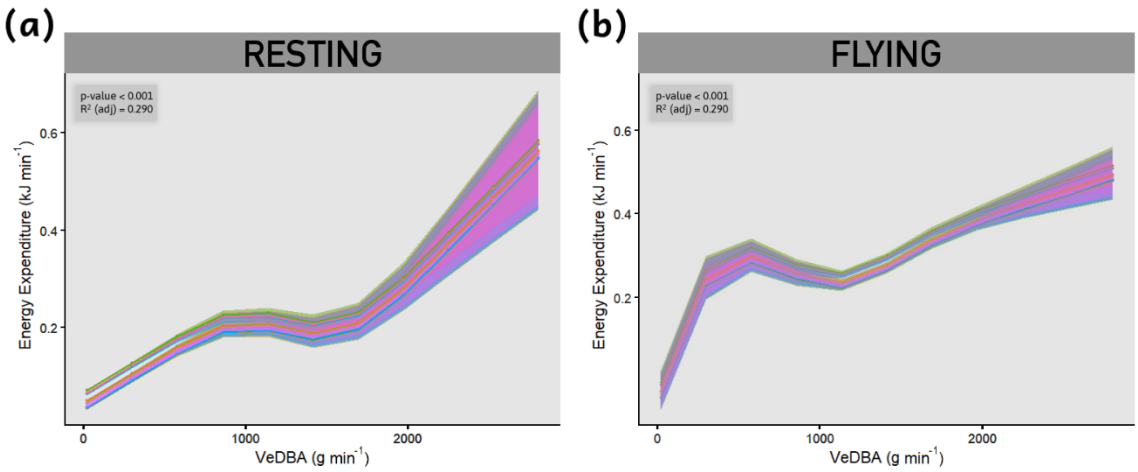

Figure 15 | Model 4. Energy expenditure (kJ min^{-1}) during rest **(a)** and during flight **(b)** relative to VeDBA. Each color represents the GAMM results for a different individual. The p-value and R^2 (adj) are shown in the upper corner for each model.

Airspeed & Energy Expenditure

To explore how energy expenditure changes with airspeed, we constructed additional generalized additive mixed effect models (GAMMs) incorporating airspeed as the independent variable (**Figure 16**). We structured the models as: *heart rate ~ airspeed*, *VeDBA ~ airspeed*, and *energy expenditure ~ airspeed*.

All of our energy metrics in each model had a negative relationship with airspeed. Heart rate and its derived energy estimate (kJ min^{-1}) had linear relationships with airspeed (**Figure 16a** - edf: 1.000; **c** - edf: 1.000). Airspeed had a larger effect on VeDBA than it did on heart rate and its derived estimate (kJ min^{-1}) (**Figure 16a** - p-value = 0.0017, t = 16.41; **(b)** - p-value < 0.001, t = 46.58; **(c)** - p-value < 0.001, t = 8.523). Airspeed also performed better at explaining the variability of VeDBA than it did for heart rate or its energy estimate (kJ min^{-1}),

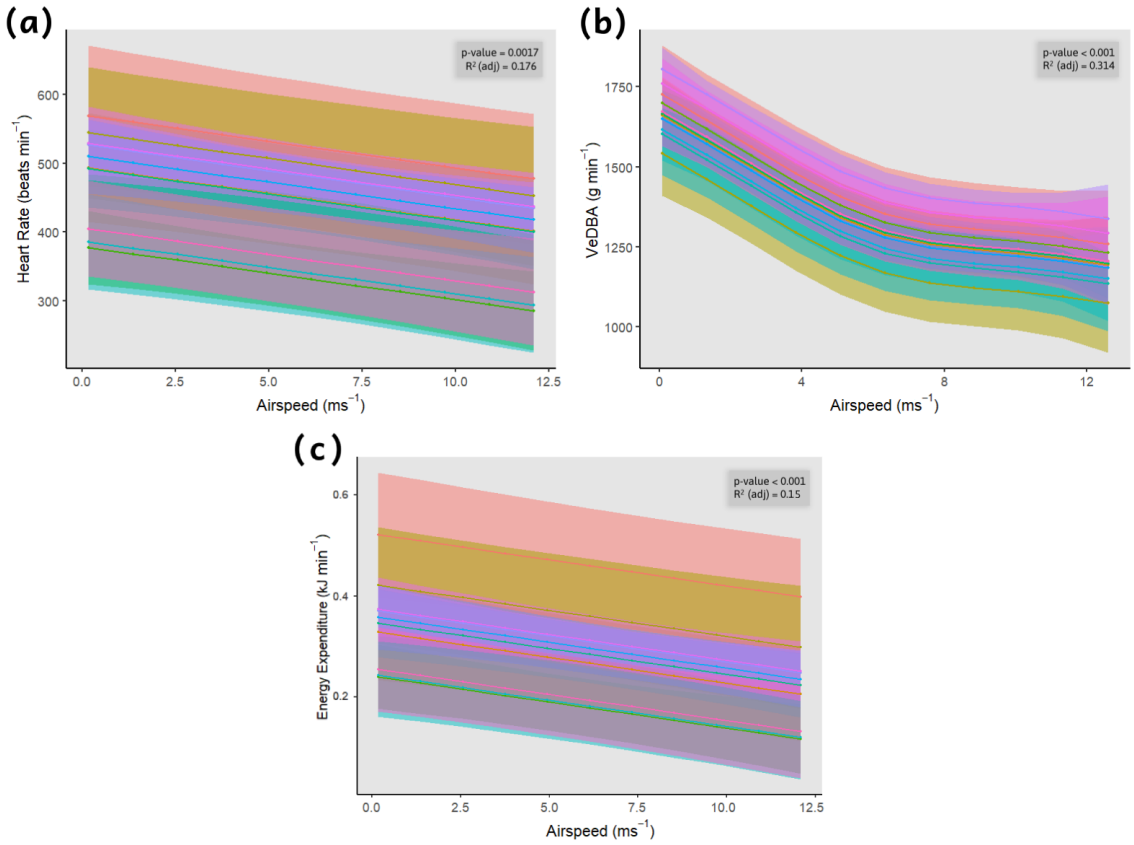

Figure 16 | Model 5-7. The effect of airspeed on different energy metrics. GAMM results are shown in color for Model 5 **(a)** heart rate, Model 6 **(b)** VeDBA, and Model 7 **(c)** energy expenditure (kJ min^{-1}). Each color represents the results for a different individual. The p-value and R^2 (adj) are shown in the upper corner for each model.

although airspeed's relationship with VeDBA was determined to be more complex (**Figure 16a** - R^2 (adj): 0.176, edf: 1.000; **(b)** - R^2 (adj): 0.314, edf: 3.011; **(c)** - R^2 (adj): 0.15, edf: 1.000). Predicting for energy expenditure (kJ min^{-1}) resulted in the lowest AIC out of all models using airspeed as the independent variable (**Figure 16a** - AIC: 3187.899; **(b)** - AIC: 11103.84; **(c)** - AIC: -208.1214).

During flight, airspeed was primarily distributed at higher and lower regions, but the majority of VeDBA and heart was distributed near their medians (**Figure 10**). We wanted to assess whether these distributions align with expected patterns based on *P. hastatus'* airspeed distribution. Using our models of airspeed (**Figure 16**), we predicted the average for each energy metric during mean flight speed.

P. hastatus flew at an average airspeed of 6.15 ms^{-1} with an average heart rate of 434.2132 ± 149.916 beats min^{-1}, an average VeDBA of 1,426.52 ± 366.46 g min^{-1}, and expended an average of 0.279 ± 0.183 kJ min^{-1}. When using airspeed as a predictor of heart rate, VeDBA and energy expenditure (kJ min^{-1}), model results predicted that while flying at their average airspeed, *P. hastatus* would have an average heart rate of 437.21 ± 65.33 beats min^{-1} (**Model 5**), an average VeDBA of 1307.1 ± 73.89 g min^{-1} (**Model 6**), and would expend an average of 0.284 ± 0.083 kJ min^{-1} (**Model 7**).

After ~220 seconds of flying, bats increased their airspeed above their minimum power speed (6.81 ± 0.21 ms^{-1}) (**Figure 17**), suggesting that *P. hastatus* may have a preferred airspeed during longer flights. Long distance flights, such as these, primarily consist of travel between roosts and foraging sites. During these types of commutes, we observed airspeed increase by 191.1%. On average, these bats flew at commuting airspeeds of 8.18 ± 2.61 ms^{-1} (**Figure 18**). The average airspeed during flights lasting less than three minutes was 2.07 ± 1.75 ms^{-1}.

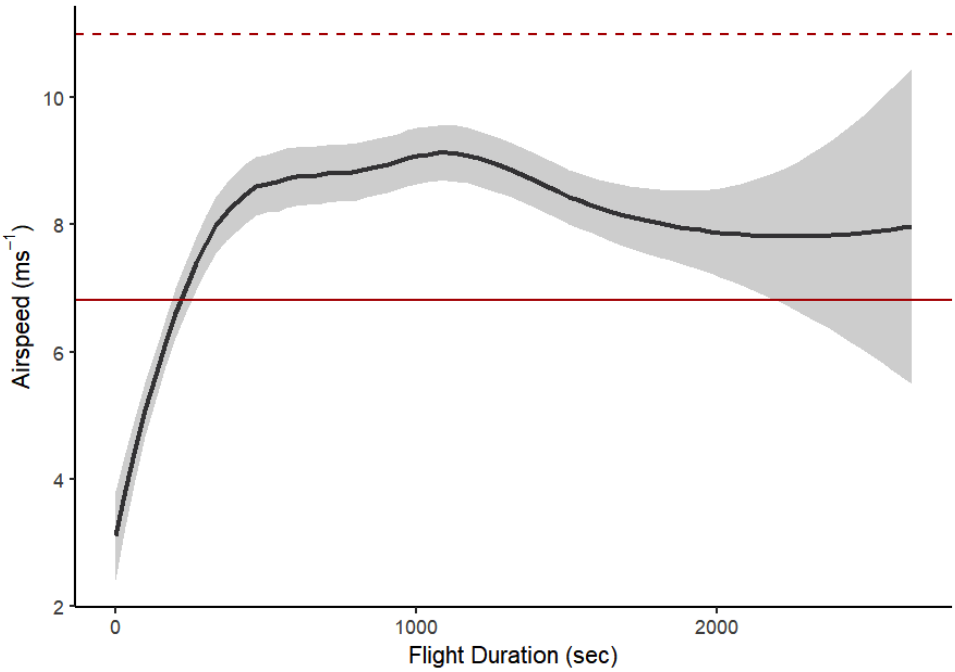

Figure 17. Average airspeed of *P. hastatus* over the duration of flight. Minimum power speed (U_{mp}) is represented by the horizontal solid red line. Maximum range speed (U_{mr}) is represented by the horizontal dashed line.

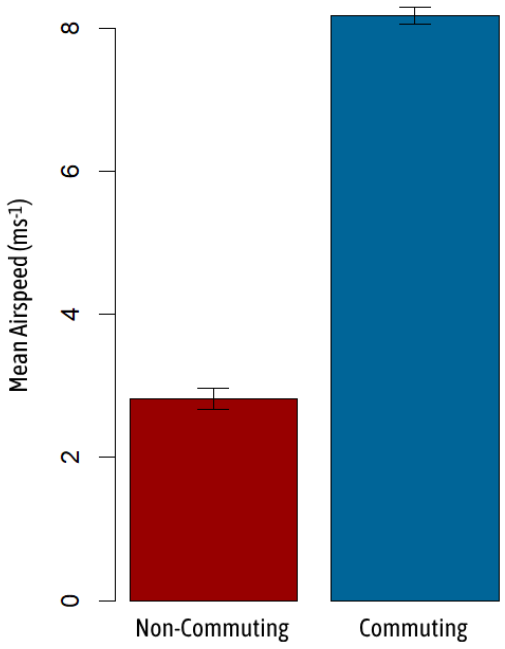

Figure 18. Bar plot comparing the average airspeeds between non-commuting and commuting flights.

To understand how airspeed patterns vary across two different flight modes, we used the duration of flight sequences as a predictor of airspeed (**Figure 19**). The relationship between airspeed and the duration of commuting flights showed a strong positive correlation, similar to that seen in **Figure 17** ($p < 0.001$). Model results also showed a positive effect of duration on airspeed during short non-commuting flights, but not statistically significant ($p = 0.235$, R^2(adj): 0.151). We observed greater variance explained in the commuting model, indicating that the duration of a flight influences the airspeed at which it is flown (**Figure 19a** - R^2(adj): 0.151, t = 7.806; **(b)** - R^2(adj): 0.213, t = 30.12).

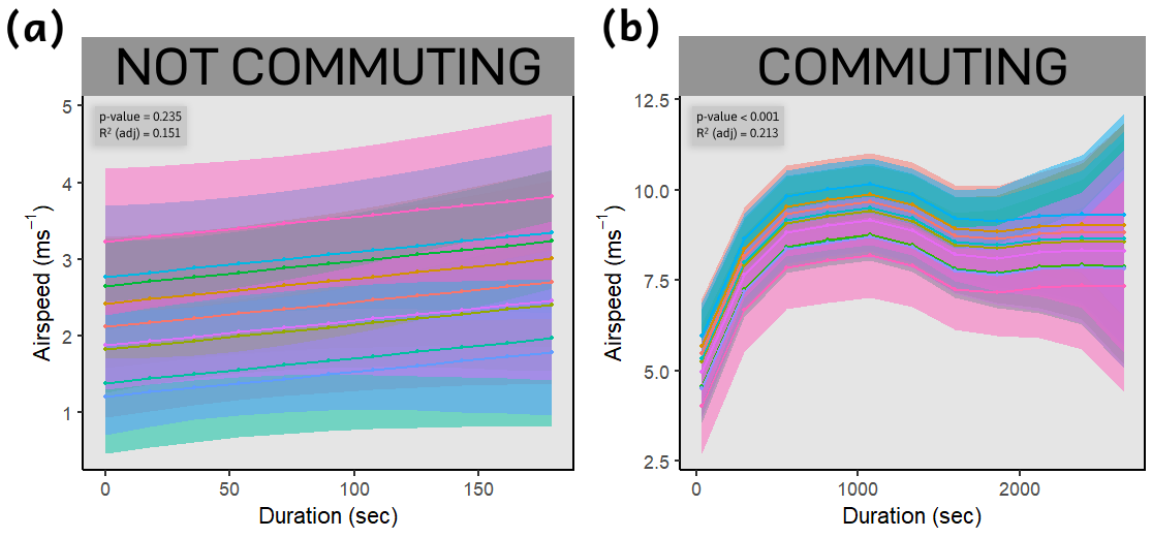

Figure 19. Airspeed during non-commuting flight **(a)** and during commuting flight **(b)** relative to the duration of it. Each color represents the GAMM results for a different individual. The p-value and R^2 (adj) are shown in the upper corner for each model.

Table 3 | GAMM results for the effect of VeDBA on heart rate and energy expenditure. The model numbers shown correlate to the model numbers in the figures above. Top performing models (Model - 2 & 4) are bolded. Additional results shown for the effect of airspeed on heart rate, energy expenditure (kJ min^{-1}), and VeDBA.

Model #	Model	Estimate	Value ± Standard error	p-value	R^2 (adj)	edf	t-value	Random effects	AIC
5	Heart rate~ Airspeed	(Intercept) Airspeed	434.68 ± 26.49	 0.0017	0.176	 1.000	16.41	Tag ID	3187.899
2	**Heart rate ~ (VeDBA): flying (VeDBA): not flying**	**(Intercept) (VeDBA): flying (VeDBA): not flying**	**224.28 ± 6.22**	** < 0.001 < 0.001**	**0.303**	** 4.596 4.885**	**36.06**	**Tag ID**	**508289.3**
1	Heart rate ~ VeDBA	(Intercept) VeDBA	225.350 ± 6.258	 < 0.001	0.301	 8.459	36.01	Tag ID	508410.8
6	Energy Expenditure~ Airspeed	(Intercept) Airspeed	0.28085 ± 0.03295	 < 0.001	0.150	 1.000	8.523	Tag ID	-208.1214
4	**Energy expenditure~ (VeDBA): flying (VeDBA): not flying**	**(Intercept) (VeDBA): flying (VeDBA): not flying**	**0.07325 ± 0.00415**	** < 0.001 < 0.001**	**0.290**	** 4.690 4.895**	**17.65**	**Tag ID**	**-123383.5**
3	Energy Expenditure ~ VeDBA	(Intercept (VeDBA)	0.074742 ± 0.004196	 < 0.001	0.286	 8.582	17.81	Tag ID	-123146.5
7	VeDBA~ Airspeed	(Intercept) Airspeed	1373.56 ± 29.49	 < 0.001	0.314	 3.011	46.58	Tag ID	11103.84

Energy Landscapes

When traveling to foraging sites, bats did not commute with groupmates. Commuting accounted for 71.66% of all flights. We observed no initial evidence of group-level cooperative foraging. Each bat used an average of 2.25 ± 0.46 foraging/resting sites located on the mainland or adjacent islands. The average foraging site was 17.47 ± 4.18 km away from the roost, while the average bat flew 17.73 ± 4.14 km to travel between each. Over 33% of this commute was flown over open ocean waters and flights to and from foraging sites were flown relatively direct, with a low average tortuosity of 1.06 ± 0.04. Each individual spent 22.38 ± 14.13% of their night flying/foraging, and 77.62 ± 14.13% resting.

Bats substantially increased their airspeeds when flying over the ocean (**Figure 20**). While flying over land, bats maintained an average airspeed of 5.48 ± 3.67 ms^{-1}, with an average heart rate of 452.71 ± 144.83 beats min^{-1} and an average VeDBA of 1446.98 ± 331.78 g min^{-1}. In contrast, while flying over the ocean, bats increased their average airspeed to 9.33 ± 1.49 ms^{-1}, with an average heart rate of 414.59 ± 133.67 beats min^{-1} and an average VeDBA of 1270.06 ± 156.63 g min^{-1}. Bats foraged and rested in separate patches of trees.

Certain GPS clusters, defined as GPS points less than 100 meters apart, were identified as just resting sites, while others were mixed-use (foraging + resting). All foraging sites had resting sites located within less than 100 m. Multiple individuals were observed returning to the same foraging and rest site on

Isla Cristóbal (Site 3) (**Table 4**). In every instance of an individual visiting the island multiple nights, they would return to the same primary foraging and resting site. Some individuals visited multiple foraging sites within the island. The average (mean ± SD) return frequency for individuals that visited Cristóbal on multiple nights was 85.5 ± 14.77 % (range: 67-100%).

Table 4. Individual foraging site information for *Phyllostomus hastatus* on Isla Cristóbal.

GPS ID	Visits to Island	Visits to Island's Foraging Sites	Returns to Same Foraging Site	Frequency (%)
Phyl33	3	4	3	75
Phyl34	2	2	2	100
Phyl38	5	5	5	100
Phyl39	2	3	2	67

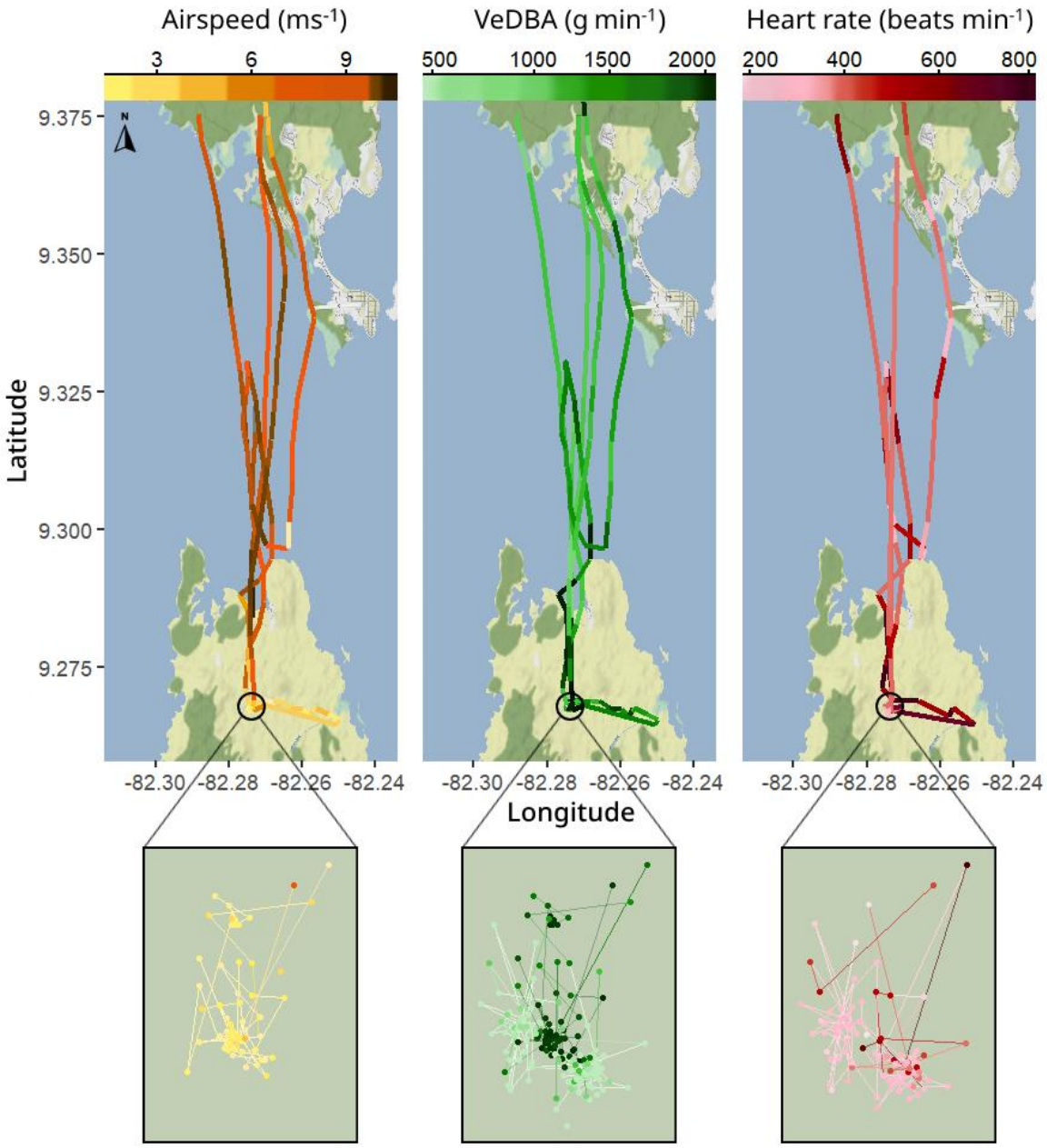

Figure 20. Distribution of a greater spear-nosed bat (GPS ID: Phyl38) foraging over an entire night. Each map represents the same movement paths, each colored according to different metrics of energy expenditure. Light colors correspond to lower values and darker colors to higher values. Insets below each map provide a scaled view of the foraging/resting patch and the bat's movements within it, each colored according to respective metrics of energy expenditure.

CHAPTER IV

DISCUSSION

By combining heart rate loggers and tri-axial accelerometers we were able to collect three different metrics of energy expenditure on 11 free-flying greater spear-nosed bats, heart rate, VeDBA, and airspeed. We found positive relationships between energy expenditure / heart rate and VeDBA that were improved through behavioral classifications of flight and rest. We also found that VeDBA was a better predictor of energy expenditure estimates derived from heart rate (kJ min^{-1}) than the raw heart rate values themselves, and that VeDBA closely resembles predictions from mechanical power curves predicted from aerodynamic theory. Our results suggest that VeDBA has a close predictive relationship with energy expenditure in bats, and that this less-invasive measure of energy expenditure and behavioral insight can be used to understand broad-scale energy expenditure and its ecological context for free-ranging bats.

When evaluating whether a proxy accurately reflects energy expenditure, it is important to test the estimate against different levels of activity. In other taxa, previous research has indicated that animals with complex relationships between their kinematics and the medium in which they travel through may benefit from increased accuracy in estimates of energy expenditure when paired with time-activity budgets (Brown et al., 2022; Jeanniard-du-Dot et al., 2016a; Jeanniard-du-Dot et al., 2017c; Ladds et al., 2017). By using a decision tree for behavioral classification (Patterson et al., 2019), we were able to classify two levels of activity, resting and flying (**Figure 6**). This behavioral classification greatly

improved the predictive fit of the VeDBA models, and revealed two different shapes in the relationship between VeDBA and heart rate and energy expenditure.

Across both behaviors we observed the positive relationship between VeDBA and heart maintained. In **Figure 9**, we can see how different levels of activity, such as resting and flying, require variable energy expenditure, and how these associated costs are sufficiently captured through each energy metric. By informing the model of the bat's behavior, we were able to better capture the variability in heart rate among the bats, across different behaviors. This was evident in the decreased slope of the resting model when compared to the flying model (**Figure 14 | Model 2**) . This implies that the relationship between VeDBA and heart rate differs depending on the bats' behavior, and while in rest, a bat's heart rate increases at a slower rate during moments of increased activity than compared to times of high, energy intensive activities such as flight.

The model displayed a steeper slope during flight, reflecting VeDBA's relationship with heart rate, which mirrored its pattern exhibited throughout flight. Initially, there was a substantial increase in heart rate corresponding to the rise in VeDBA, followed by a brief decline before stabilizing or gradually increasing, similar to the observed pattern at the onset of flight (**Figure 21**). This is most likely indicative of the initial energy intensive act of taking flight, which might not result in as much VeDBA as it does require oxygen delivery via increased heart rate.

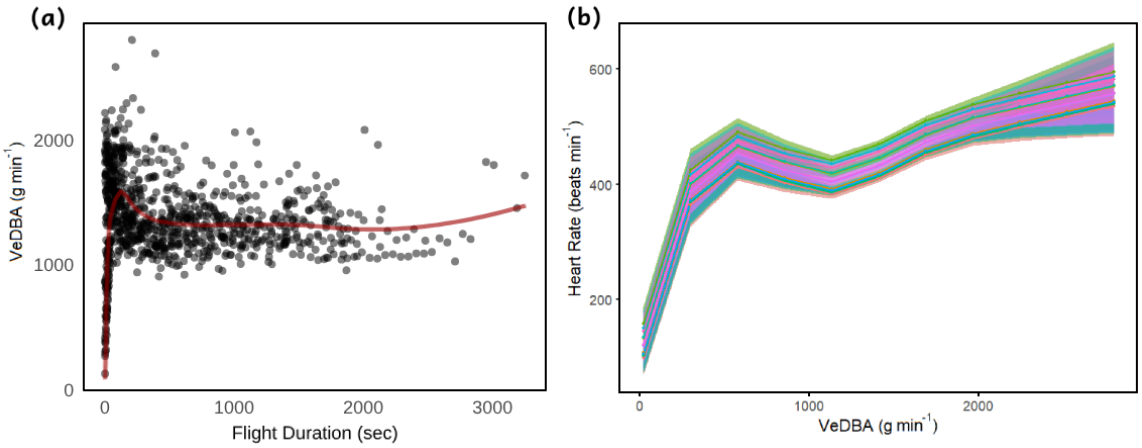

Figure 21 (a) - The distribution of VeDBA and its pattern from the start of flight throughout its duration, with the red LOESS line depicting the general trend of the data. **(b)** Heart rate during flight relative to VeDBA.

We saw the positive relationship between heart rate and VeDBA further improved by replacing the dependent variable (heart rate) in our behaviorally classified model (**Model 2**) with the heart rate-derived estimate of energy expenditure (kJ min^{-1}) (**Model 3 & 4)**. This also provides further support for the method of behaviorally classifying the models when we compared the goodness-of-fit, complexity of the smooth terms, and how well VeDBA explained the variability in energy expenditure from **Model 3** and **Model 4**.

By using VeDBA as a predictor of energy expenditure (kJ min^{-1}), we also showed VeDBA to represent a quality indicator of oxygen consumption, providing further support for its use as an estimation of energy expenditure in bats (**Model 3**). However, muscle efficiency can differ between levels of activity (Gómez Laich et al., 2011) which may cause changes in the relationship between oxygen consumption and accelerometry, so new models were constructed, accounting for behavior. Behaviorally classified models showed a positive relationship

between VeDBA and energy expenditure (kJ min^{-1}) (**Model 4**). Although the relationship between energy expenditure (kJ min^{-1}) and VeDBA varied between behaviors, it closely mirrored the relationship seen between heart rate and VeDBA (**Model 2**).

When comparing VeDBA to various measures of energy expenditure, it is important to understand the fundamentals of each and how they are measured. As a result of a resting metabolic rate, heart rate never drops to zero. In situations where there is no movement (such as during sleep or inactivity), VeDBA can approach or reach zero, indicating minimal body acceleration. There is also a delay in the response of heart rate to changes in activity levels. It's also important to consider the range of scale sizes for each metric. Within our study, VeDBA is calculated on a much larger scale (range: 22.45-3023.74 g min^{-1}) compared to the measurement scale of heart rate (range: 101-800 beats min^{-1}). These fundamental differences in their baselines and dynamics affect how they are compared and are key factors to consider when using either of them as proxies of energy expenditure.

When selecting which models performed the best, we prioritized values of AIC then R^2. We found VeDBA served as a better predictor for energy expenditure (kJ min^{-1}) than heart rate and had substantially lower AIC values (**Model 1** - AIC: 508410.8; **Model 3** - AIC: -123146.5). The benefit of using energy expenditure (kJ min^{-1}) as the dependent variable might result from incorporating individualized morphometric measures (M_b, M_h) in $\dot{V}O_2$ estimation (**Eq. 4**). Additionally, R^2(adj) was slightly higher in models when VeDBA predicted

heart rate, suggesting VeDBA was better at explaining the variability of heart rate than energy expenditure (kJ min^{-1}) (**Model 1** - R^2(adj): 508410.8; **Model 3** - R^2(adj): -123146.5). We also found behaviorally classifying models to provide multiple statistical improvements in the performance of the model, which was most evident in **Model 2**. Interestingly, by incorporating behavior into models, edf values dropped by almost half, which suggests that information on activity levels decreases the complexity of VeDBA's relationship with each metric of energy expenditure. Based on these model results, we concluded that **Model 4** performed the best. While **Model 2** had a higher AIC value than Model 3 & 4, it had a slightly larger R^2(adj). It also performed better in all other statistical analyses. As a result, we determined **Model 2** to be the next best fit.

The airspeed at which a bat chooses to fly should be strongly linked to the mechanical power and energy required to maintain that speed (Hedenström and Alerstam; 1996; Hedenström and Thomas, 1995; O'Mara and Dechmann, 2023; Pennycuick, 2008; Pennycuick, 1975; von Busse et al., 2013). Previous work has estimated the minimum power speed (6.81 ± 0.21 ms^{-1}) and maximum range speed (11.0 ± 0.35 ms^{-1}) for greater spear-nosed bats, establishing a framework for understanding the power requirements of various flight speeds (O'Mara & Dechmann, 2023). Based on this, during times of low airspeed, we expected an increase in the power required to stay in the air. Conversely, as airspeeds increased up to their estimated maximum range speed, we expected to see a decrease in the power required to maintain flight.

We demonstrated that increasing airspeed is associated with decreasing flight power across all three metrics of energy expenditure using GAMMs. Using AIC and R^2(adj) as a selection tool, we concluded that airspeed was able to best predict energy expenditure (kJ min^{-1}) and VeDBA (**Table 3**). Using the distributions of each energy metric during flight, we verified the accuracy of each airspeed model, providing evidence for a strong relationship between airspeed and energy expenditure. Flying at a maximum airspeed of ~12 ms^{-1}, the observed power curves correspond to the initial segment of *P. hastatus'* predicted power curve (**Figure 22**). Aerodynamic theory predicts that it is most energetically efficient to fly between the minimum power speed and the maximum range speed (Pennycuick, 2008; Pennycuick, 1975; Rayner, 1979; Tucker, 1974). The power required to maintain flight is a combination of the power needed to overcome both induced and parasite drag. At low speeds, high induced drag demands more power. As speed increases, induced drag decreases, minimizing power needs at a specific point (minimum power speed). Beyond this, parasite drag, which grows with the square of speed, dominates and rapidly raises power requirements. Maximum range speed optimizes the balance between induced and parasite drag, maximizing distance per unit of energy. Beyond this speed, increased parasite drag significantly reduces energy efficiency due to higher power demands (Pennycuick, 2008; Pennycuick, 1975). The maximum airspeed flown by *P. hastatus* during this study was 12.59 ms^{-1}, indicating that these bats rarely exceeded their estimated maximum range speeds (11.0 ± 0.35 ms^{-1}).

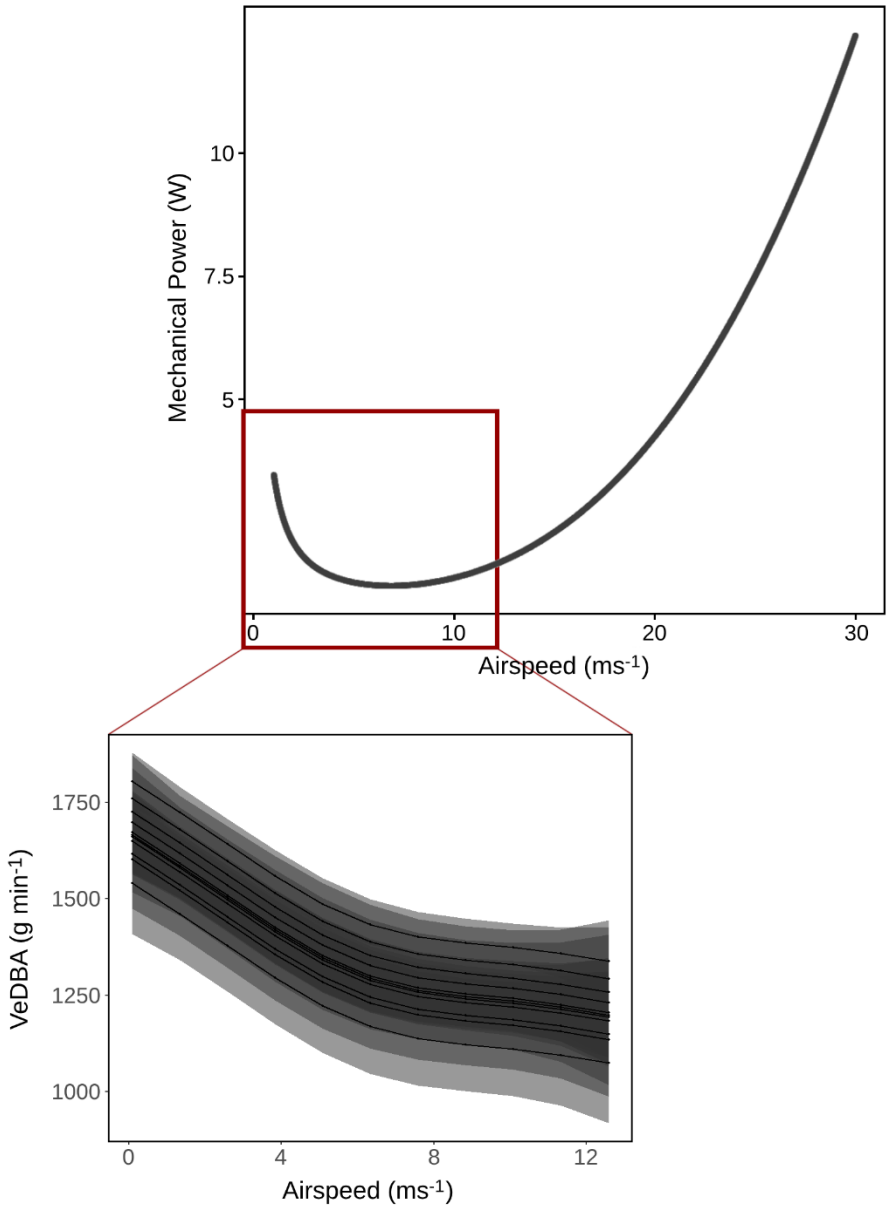

Figure 22. The estimated power curve of greater spear-nosed bats (top), with an inset of the observed energy expenditure of *P. hastatus* across various flight speeds. The red box represents the general position of the observed energy costs relative to the entire power curve estimate.

Based on this, and our model results (**Figure 16 | Model 5-7**), we concluded that flight speeds of *P. hastatus* closely followed the previously estimated mechanical power curves for this species (**Figure 22**).

Characterizing *P. hastatus'* power curve provides a way to practically assess their biomechanical and physiological capabilities, valuable for comparing flight patterns and route selection, and offers a mechanistic perspective on decisions regarding flight speed and optimal foraging strategies (Grodzinski et al., 2009; Hedenström and Alerstam; 1996; Hedenström and Thomas, 1995; O'Mara and Dechmann, 2023; Pennycuick, 2008; Pennycuick, 1975; von Busse et al., 2013).

We also hypothesized that bats would primarily fly within energetically optimal flight speeds. Since flying within the estimated minimum power speed and maximum range speed is the least energetically expensive for *P. hastatus* (O'Mara and Dechmann, 2023), we anticipated that these bats would increase their airspeed above the minimum power speed shortly after taking off for the majority of flights. Using LOESS smoothing, we created a scatter plot to reveal how airspeed changes throughout the duration of all flight data (**Figure 17**). Bats increased their airspeed above the minimum power speed within the first ~3 minutes of flight and maintained it above the minimum power speed but below the maximum range speed throughout the flight. We concluded that the majority of flights were flown at an energetically optimal airspeed.

To understand how airspeeds are distributed across short and long-distance flights, we used the duration of flight to predict changes in airspeed (**Figure 19**). Model results showed that commuting airspeed is strongly related to how long the flight lasts, suggesting that bats may modulate their flight speeds based on the anticipated travel distance or time. To increase energy efficiency,

the majority of long flights, such as commuting journeys between roosting sites and foraging grounds, should be flown within this energetically optimal range. This movement-based decision would reflect the optimization of energy expenditure over extended time and space. Bats may adjust their flight dynamics to achieve a balance between covering distance quickly and conserving energy to sustain flight. In contrast, shorter flights, which typically involve local movements or brief foraging trips, exhibit more variable or lower average airspeeds. While model results showed a positive relationship between non-commuting airspeed and the duration of the flight, it was not statistically significant. This means there's no strong evidence to suggest that these bats prioritize the energetic benefits gained from flying at increased airspeeds during short bouts of flight. These shorter flights may prioritize immediate task completion or navigation within the surrounding environment, allowing for greater maneuverability and turning agility. The variability in airspeed across flight types may reflect adaptive strategies to the specific energetic demands and locomotor challenges encountered during different behaviors (von Busse et al., 2014).

Animals are continuously expending energy, and therefore do so as a function of time (Wilson et al., 2012). How energy expenditure gets distributed over a temporal scale is best illustrated in **Figure 8**. However, the associated metabolic costs vary according to the precise method in which it is expended (Wilson et al., 2012). When plotted over 24 hours, we can see that the distribution of VeDBA broadly mirrors the changes in heart rate. High levels of activity occur exclusively during nighttime hours, with no flight observed during

the daytime (see black bars in **Figure 8**). Nightly energy expenditure, averaged across all bats, was characterized by three large peaks in heart rate and VeDBA. These likely correspond to average time of emergence, a major foraging event, and the return trip to the roost. This would suggest that during foraging there is, to some degree, a temporal distribution pattern to energy expenditure across a social group or possibly roost.

The spatial and temporal distribution of energy expenditure plays a pivotal role in determining the quality of a foraging patch and daily energy requirements, which shapes the distribution and abundance of wildlife populations (Shepard et al., 2013; Stephens and Krebs, 1986; Wilson et al., 2012). For animals, movement incurs both energy-related costs and benefits, and examining their use of the landscape provides a perspective into their decision-making and behavioral ecology. When and where animals expend their energy is a direct result of the interaction between their movement decisions and the landscape they live in (Shepard et al., 2013; Wilson et al., 2012). Landscapes vary in character, such as changes in the medium through which the animal travels, including changes in wind speed and direction, or moving from an open area into a dense forest, which can make movement more challenging (Wilson et al., 2012). Landscapes also change over time; for example, resource availability can vary across seasons. The degree of variation in the landscape influences movement costs, this variation translates into dynamic movement decisions and energy costs for animals traveling through it (Wilson et al., 2012).

Using GPS, accelerometry, and heart rate data metrics, we selected a bat (GPS ID: Phyl38) with high-quality data to model how greater spear-nosed bats distribute their energy expenditure throughout a foraging night. This model illustrates a strong relationship between terrain and movement preferences. While flying over the ocean, bats would increase their airspeed by 70.26% which resulted in a 17.24% decrease in energy expenditure (kJ min^{-1}). During this time, airspeeds were maintained above the minimum power speed and maximum range speed. However, non-commuting flights averaged much lower airspeeds, indicating that *P. hastatus* does not consistently maintain this energetic optimum. Changes in airspeed may represent a method of balancing trade-offs between costs and rewards during foraging nights. Due to the increased maneuverability required from foraging in dense vegetation, bats may exhibit higher energy expenditure flying over land, compared to more open areas such as over the ocean, where flight may be less energetically demanding to navigate (Shepard et al., 2013). This suggests that these bats use adjustments to airspeed as an energy-saving strategy depending on the distance to be traveled or the purpose of the flight.

As bats approached the western coastline of Bocas del Toro, many individuals were observed making slight deviations in their trajectory, following the path of the coast before eventually heading towards their destination. It is unclear whether bats used these coastlines as a roadmap or landmark to guide them towards their intended destination, or if there is an energetic benefit gained from this behavior. Further work is needed to model potential relationships

between wind speed, wind direction, and energy expenditure along this path to better understand this pattern.

Greater spear-nosed bats are known to have a diverse diet throughout the year, but switch almost exclusively to *O. pyramidale* during the dry season (O'Mara and Dechmann, 2023). Previous work on bats from the same roost has shown that while *P. hastatus* commuted and often foraged alone, some individuals reunited with other group members at these flower patches. Individuals from our study commuted and foraged completely alone. These species all travel from a shared roost to distant foraging patches, yet we observed no overlap in individual foraging ranges among group members. These distinct ranges may have developed through reinforcement learning processes aimed at reducing competition (Goldshtein et al., 2020; O'Mara and Dechmann, 2023). This also may be influenced by seasonal changes to their resource distribution and food type, as well as the dynamic value of social information during these shifts (Kohles et al., 2022; O'Mara and Dechmann, 2023). It is likely that there is also a degree of plasticity in foraging behaviors across social groups and seasons (Boughman, 2006). Social group formations and foraging strategies may also vary regionally or across populations depending on the resource landscape. In Trinidad, females forage in groups depending on the season. They use special group-specific social calls to form foraging groups (Boughman, 1998; Wilkinson and Boughman, 1998). It has been suggested that recruiting group members to foraging patches could serve as a strategy to defend trees against competitors (Wilkinson and Boughman, 1998). Further work mapping their

resource landscape across seasons is needed to better understand how seasonal changes to it affect energy expenditure, movement patterns, and foraging strategies.

Other species of bats that feed on nectar and fruit seem to possess extensive and well-developed cognitive maps of their foraging territories (Harten et al., 2020; Toledo et al., 2020). These bats demonstrated substantially high return rates to specific foraging sites, and flights to and from these foraging sites showed low tortuosity, indicating that these animals do not distribute themselves randomly and exhibit relatively high spatial cognition. Low degrees of exploratory behavior while foraging can indicate predictable sources of food at high quality food patches (Stephens and Krebs, 1986). In general, these bats would forage in a patch of trees and then rest in another close by (**Figure 20**). They did not forage and rest in the same patch of trees. How their food is distributed is likely a significant driver of these movement choices and foraging behaviors.

Ultimately, measuring the energetic costs of movement across landscapes offers a mechanistic understanding of animal-based decision-making important to advancing movement ecology (Bishop et al.,. 2015; Elliott et al., 2013; Gleiss et al., 2011; Gómez Laich et al., 2011; Green et al., 2008; Hicks et al., 2017; Stothart et al., 2016; Sutton et al., 2023; Wilson et al., 2020; Wilson et al., 2012). This provides a perspective into how and why animals distribute themselves across space and time (Bishop et al.,. 2015; Klappstein et al., 2022; O'Mara et al., 2021; Scacco, 2021; Shepard et al., 2013), especially those living at their metabolic ceiling and rely on ephemeral resources like *P. hastatus*.

Measuring field energy expenditure offers insights into the metabolisms of animals, and provides valuable ecological insight into metabolic requirements and physiological limitations, revealing how they acclimatize to environmental changes such as temperature fluctuations, food scarcity, or habitat alterations (Bishop et al., 2015; Castejón-Silvo et al., 2021; Elliott et al., 2013; Watanabe et al., 2020). Knowing when and where an animal is expending energy helps identify metabolically valuable spatial or temporal areas within an animal's environment which can ultimately be used to improve conservation strategies (Madliger et al., 2020; Wikelski and Cooke, 2006). This study has provided support for the use of VeDBA as a less-invasive method for measuring energy expenditure, capable of providing behavioral insight that can be used to understand broad-scale energy distribution and its ecological context for free-ranging bats.

SUPPLEMENTARY MATERIALS

Table 5. Definitions of accelerometry-derived metrics, statistics, and other variables of energy expenditure used.

Variable	Units	Meaning
A_X, A_Y, A_Z	ms^2	Raw acceleration of each axis
S_X, S_Y, S_Z	ms^2	Static acceleration of each axis
θ	°	Pitch angle
D_X, D_Y, D_Z	ms^2	Dynamic acceleration of each axis
VeDBA	g min^{-1}	Vectorial Dynamic Body Acceleration
$\bar{X}$ $VeDBA_F$	g min^{-1}	Mean rate of estimated energy expenditure during flight
EE_{hr}	kJ min^{-1}	Heart rate-derived estimate of energy expenditure
$\bar{X}$ EE_F	kJ min^{-1}	Mean rate of energy expenditure during flight
DEE	kJ day^{-1}	Total daily energy expenditure
X, Y, Z	ms^2	Axes of acceleration in three perpendicular planes
$\dot{V}O_2$	ml min^{-1}	Rate of oxygen consumption
$\bar{X}$ $\dot{V}O_{2\,F}$	ml min^{-1}	Mean rate of oxygen consumption during flight
M_b	kg	Body mass
M_h	kg	Heart mass
f_H	beats min^{-1}	Heart beat frequency
U_{mp}	ms^{-1}	Minimum power speed
U_{mr}	ms^{-1}	Maximum range speed

DATA AVAILABILITY

The data sets analyzed during this study are available in the Movebank Data Repository under study name: Greater spear-nosed bats (*Phyllostomus hastatus*) in Bocas del Toro 2023.

FUNDING

This study was supported by the U.S. National Science Foundation (Award Number: 2217920).

STUDY ACKNOWLEDGEMENTS

We thank the owners of Cueva La Gruta for access to the research site, Steve Patton, Milton Solano and the Smithsonian Tropical Research Institute for assistance with logistics and support, as well as Plinio Gondola and Urania González from the Bocas station for their services, resources and research facilities. We would like to also thank James Lee, Leslye Barría, and Luisa Fernanda for help in the field, and Graciela Aguilar for veterinary assistance.

REFERENCES

Algar, A.C., Kerr, J.T. and Currie, D.J. (2007). A test of Metabolic Theory as the mechanism underlying broad-scale species-richness gradients. *Global Ecology and Biogeography*, 16: 170-178. doi: 10.1111/j.1466-8238.2006.00275.x

Andersson, K. & Werdelin, L. (2003). The evolution of cursorial carnivores in the Tertiary: implications of elbow-joint morphology. *Proceedings of the Royal Society of London. Series B: Biol. Sci.* 270(2), S163-S165. doi: 10.1098/rsbl.2003.0070

Andrewartha, H. G. and Birch, L. C. (1954). The distribution and abundance of animals. (No. Edn 1, pp. 782)

Anholt, B. R. and Werner, E. E. (1995). Interaction between food availability and predation mortality mediated by adaptive behavior. *Ecology.* 76(7):2230–2234.

Auer, S. K., Solowey, J. R., Rajesh, S., Rezende, E. L. (2020). Energetic mechanisms for coping with changes in resource availability. *Biol Lett.* 16(11):20200580. doi: 10.1098/rsbl.2020.0580

Barske, J., Fusani, L., Wikelski, M., Feng, N. Y., Santos, M., Schlinger, B. A. (2014). Energetics of the acrobatic courtship in male golden-collared manakins (*Manacus vitellinus*). *Proc. R. Soc. B.* 281:1776. doi: 10.1098/rspb.2013.2482

Bergmüller, R., Schürch, R., Hamilton, I.M. (2010). Evolutionary causes and consequences of consistent individual variation in cooperative behaviour. *Philos Trans R Soc Lond B Biol Sci.* 365(1553):2751-64. doi: 10.1098/rstb.2010.0124

Bidder, O. R., Goulding, C., Toledo, A., van Walsum, T. A., Siebert, U. and Halsey, L. G. (2017). Does the treadmill support valid energetics estimates of field locomotion? *Int. Comp. Bio.*, 57, 301–319.

Bishop, C. M. & Spivey, R. J. (2013). Integration of exercise response and allometric scaling in endotherms. *Journal of Theoretical Biology.* 323:11–19. doi: 10.1016/j.jtbi.2013.01.002

Bishop, C. M., Spivey, R. J., Hawkes, L. A., Batbayar, N., Chua, B., Frappell, P. B., Milsom, W. K., Natsagdorj, T., Newman, S. H., Scott, G. R., Takekawa, J. Y., Wikelski, M., & Butler, P. J. (2015). The roller coaster flight strategy of bar-headed geese conserves energy during Himalayan migrations. *Science*, *347*(6219), 250–254. doi: 10.1126/science.1258732

Boughman, J. W. (1998). Vocal learning by greater spear-nosed bats. *Proc. R Soc. B.*, 265(1392), 227–233. doi: 10.1098/rspb.1998.0286

Boughman, J. and Wilkinson, G. (1998). Greater spear-nosed bats discriminate group mates by vocalizations. *Anim. Behav.* 55(6), 1717–1732. doi: 10.1006/anbe.1997.0721

Boughman, J. W. (2006). Selection on social traits in greater spear-nosed bats, *Phyllostomus hastatus*. *Behav. Ecol. Sociobiol.* 60, 766-777.

Bowlin, M. S., Cochran, M. W., Wikelski, M. C. (2005). Biotelemetry of New World thrushes during migration: Physiology, energetics and orientation in the wild. *Int. Comp. Biol.*, 45(2), 295–304. doi: 10.1093/icb/45.2.295

Bozinovic, F., Muñoz, J. L. P., Naya, D. E., Cruz-Neto, A. P. (2007). Adjusting energy expenditures to energy supply: food availability regulates torpor use and organ size in the Chilean mouse-opossum *Thylamys elegans*. *J. Comp. Phys. B.* 177(4), 393-400. doi: 10.1007/s00360-006-0137-0

Bro-Jørgensen, J. (2013), EVOLUTION OF SPRINT SPEED IN AFRICAN SAVANNAH HERBIVORES IN RELATION TO PREDATION. *Evolution*, 67: 3371-3376. doi: 10.1111/evo.12233

Brose, U., Ehnes, R. B., Rall, B. C., Vucic-Pestic, O., Berlow, E. L. and Scheu, S. (2008). Foraging theory predicts predator–prey energy fluxes. *Journal of Animal Ecology*, 77: 1072-1078. doi: 10.1111/j.1365-2656.2008.01408.x

Brown, J. M., Bouten, W., Camphuysen, K. C. J., Nolet, B. A. and Shamoun-Baranes, J. (2022). Acceleration as a proxy for energy expenditure in a facultative-soaring bird: Comparing dynamic body acceleration and time-energy budgets to heart rate. *Functional Ecology*, 36:1627–1638. doi: 10.1111/1365-2435.14055

Brown, J. M., Bouten, W., Camphuysen, K. C. J., Nolet, B. A. and Shamoun-Baranes, J. (2023). Energetic and behavioral consequences of migration: an empirical evaluation in the context of the full annual cycle. *Sci Rep,* 13,1210. doi: 10.1038/s41598-023-28198-8

Brown, D. D., Kays, R., Wikelski, M. et al. (2013). Observing the unwatchable through acceleration logging of animal behavior. *Anim Biotelemetry,* 1, 20. doi: 10.1186/2050-3385-1-20

Brown J. H., Gillooly J. F., Allen A. P., Savage V. M. and West G. B. (2004). Toward a metabolic theory of ecology. *Ecology,* 85, doi: 1771-1789. 10.1890/03-9000

Butler, P. J., Green, J. A., Boyd, I. L. and Speakman, J.R. (2004). Measuring metabolic rate in the field: the pros and cons of the doubly labelled water and heart rate methods. *Functional Ecology*, 18: 168-183. doi: 0.1111/j.0269-8463.2004.00821.x

Canals, M., Atala, C., Grossi, B., Iriarte-Díaz, J. (2005). Relative Size of Hearts and Lungs of Small Bats. *Acta Chiropterologica* 7:1, 65–72. doi: 10.3161/1733-5329

Cant, J. P., McBride, B. W. and Croom Jr, W. J. (1996). The regulation of intestinal metabolism and its impact on whole animal energetics. *Journal of animal science,* 74(10), 2541-2553

Caspi, T., Johnson, J. R., Lambert, M. R., Schell, C. J., Sih, A. (2022). Behavioral plasticity can facilitate evolution in urban environments. *Trends Ecol Evol.* 37(12):1092-1103. doi: 10.1016/j.tree.2022.08.002

Castejón-Silvo, I., Terrados, J., Nguyen, T., Jutfelt, F., and Infantes, E. (2021). Increased energy expenditure is an indirect effect of habitat structural complexity loss. *Functional Ecology*. 35, 2316–2328. doi: 10.1111/1365-2435.13876

Chakravarty, P., Cozzi, G., Ozgul, A., Aminian, K., O'Hara, R. B. (2019). A novel biomechanical approach for animal behaviour recognition using accelerometers. *Methods Ecol. Evol.* 10, 802-814. doi: 10.1111/2041-210x.13172

Dawkins, R., and J. R. Krebs. (1979). Arms races between and within species. *Proc. R. Soc. Lond. Biol. Sci.* 205: 489–511

Dickinson, E. R., Stephens, P. A., Marks, N. J. Wilson, R. P. and Scantlebury, D. M. (2021). Behaviour, temperature and terrain slope impact estimates of energy expenditure using oxygen and dynamic body acceleration. *Anim Biotelemetry,* 9(47) doi: 10.1186/s40317-021-00269-5

Dickinson, M. H., Farley, C. T., Full, R. J., Koehl, M. A. R., Kram, R., Lehman, S. (2000). How animals move: an integrative view. *Science,* 288(5463), 100–106. doi: 10.1126/science.288.5463.100

Dunford, C. E., Marks, N. J., Wilmers, C. C., Bryce, C. M., Nickel, B., Wolfe, L. L. et al. (2020). Surviving in steep terrain: a lab-to-field assessment of locomotor costs for wild mountain lions (*Puma concolor*). *Mov Ecol.* 8:34. doi: 10.1186/s40462-020-00215-9

Elliott, K. H. (2016). Measurement of flying and diving metabolic rate in wild animals: review and recommendations. *Comp. Biochem. Physiol. A Mol. Integr. Physiol.* 202, 63–77. doi: 10.1016/j.cbpa.2016.05.025

Elliott, K. H., Le Vaillant, M., Kato, A., Speakman, J. R., and Ropert-Coudert, Y. (2013). Accelerometry predicts daily energy expenditure in a bird with high activity levels. *Bio. Lett.* 9:20120919. doi: 10.1098/rsbl.2012.0919

Engel, S., Bowlin, M. S., Hedenström, A. (2010). The role of wind-tunnel studies in integrative research on migration biology. *Integr. Comp. Biol.* 50, 323–335. doi: 10.1093/icb/icq063

Enstipp, M. R., Ciccione, S., Gineste, B., Milbergue, M., Ballorain, K., Ropert-Coudert, Y. et al. (2011). Energy expenditure of freely swimming adult green turtles (*Chelonia mydas*) and its link with body acceleration. *J Exp Bio*, 214:322 4010-4020.

Forsman, A. and Wennersten, L. (2016), Inter-individual variation promotes ecological success of populations and species: evidence from experimental and comparative studies. *Ecography*, 39: 630-648. doi: 10.1111/ecog.01357

Frey-Roos, F. Brodmann, P. A. and Reyer, H. (1995). Relationships between food resources, foraging patterns, and reproductive success in the water pipit, *Anthus sp. spinoletta*. *Behavioral Ecology*, 6(3), 287–295. doi: 10.1093/beheco/6.3.287

Geiser, F. (1988). Reduction of metabolism during hibernation and daily torpor in mammals and birds: temperature effect or physiological inhibition?. *Journal of Comparative Physiology B*, 158(1), 25-37.

Geiser, F. (2004). Metabolic rate and body temperature reduction during hibernation and daily torpor. *Annu Rev Physiol*. 66:239-74. doi: 10.1146/annurev.physiol.66.032102.115105

Geiser, F. (2019). Hibernation, Daily Torpor and Estivation in Mammals and Birds: Behavioral Aspects. *Encyclopedia of Animal Behavior* 2:2, 571-578. doi: 10.1016/B978-0-08-045337-8.00247-3

Geiser, F., Wen, J., Sukhchuluun, G., Chi, Q. S. and Wang D. H. (2019). Precocious torpor in an altricial mammal and the functional implications of heterothermy during development. *Front Physiol,* 10:469. doi: 10.3389/fphys.2019.00469

Giraldeau, L. A. and Beauchamp, G. (1999). Food exploitation: searching for the optimal joining policy. *Trends Ecol Evol.* 14(3):102-106. doi: 10.1016/s0169-5347(98)01542-0

Gleiss, A. C., Wilson, R. P. & Shepard, E. L. C. (2011). Making overall dynamic body acceleration work: on the theory of acceleration as a proxy for energy expenditure. *Methods Ecol. Evol*. 2, 23–33. doi: 10.1111/j.2041-210X.2010.00057.x

Goldshtein, A., Handel, M., Eitan, O., Bonstein, A., Shaler, T., Collet, S., Greif, S., Medellín, R. A., Emek, Y., Korman, A., and Yovel, Y. (2020). Reinforcement learning enables resource partitioning in foraging bats. *Current Biology*, 30(20), 4096e4102. doi: 10.1016/j.cub.2020.07.079

Gómez Laich, A., Wilson, R. P., Gleiss, A. C., Shepard, E. L. C. and Quintana, F. (2011). Use of overall dynamic body acceleration for estimating energy expenditure in cormorants. *J. Exp. Mar. Biol. Ecol.* 399, 151-155. doi: 10.1016/j.jembe.2011.01.008

Gray, J. (1968). *Animal locomotion*. Weidenfeld & Nicolson.

Green, J. A., Halsey, L. G., Wilson, R. P, & Frappell, P. B. (2008). Estimating energy expenditure of animals using the accelerometry technique: activity, inactivity and comparison with the heart-rate technique. *J. Exp. Biol.* 212, 471–482. doi:10.1242/jeb.026377

Green, J. A., Boyd, I. L., Woakes, A. J., Warren, N. L., & Butler, P. J. (2009). Evaluating the Prudence of Parents: Daily Energy Expenditure throughout the Annual Cycle of a Free-Ranging Bird, the Macaroni Penguin *Eudyptes chrysolophus*. *Journal of Avian Biology*, 40(5), 529–538.

Green, J. A. (2011). The heart rate method for estimating metabolic rate: Review and recommendations, *Comp Biochem and Phys Part A: Molec & Int Phys*, 158(3), 287-304. doi: 10.1016/j.cbpa.2010.09.011

Grodzinski, U., Spiegel, O., Korine, C. and Holderied, M.W. (2009). Context-dependent flight speed: evidence for energetically optimal flight speed in the bat *Pipistrellus kuhlii*?. *Journal of Animal Ecology*, 78: 540-548. doi: 10.1111/j.1365-2656.2009.01526.x

Halsey L. G., Shepard E. L. C., Quintana F., Gomez Laich A., Green J. A. and Wilson R. P. (2009). The relationship between oxygen consumption and body acceleration in a range of species. *Comp. Biochem. Physiol. A Mol. Integr. Physiol.* 152, 197-202. doi: 10.1016/j.cbpa.2008.09.021

Harten, L., Katz, A., Goldshtein, A., Handel, M., & Yovel, Y. (2020). The ontogeny of a mammalian cognitive map in the real world. *Science*, 369(6500), 194e197. doi: 10.1126/science.aay3354

Hedenström, A. and Thomas, A. (1995). Optimal flight speed of birds. *Phil. Trans. R. Soc. Lond.* B348471–487 doi: 10.1098/rstb.1995.0082

Hedenström, A. and Alerstam, T. (1996). Skylark optimal flight speeds for flying nowhere and somewhere. *Behav. Ecol.* 7(2), 121-126. doi: 10.1093/beheco/7.2.121

Hicks, O., Burthe, S., Daunt, F., Butler, A., Bishop, C., Green, J. A. (2017). Validating accelerometry estimates of energy expenditure across behaviours using heart rate data in a free-living seabird. *J Exp Biol.* 15;220(Pt 10):1875-1881. doi: 10.1242/jeb.152710

Hirt, M. R., Jetz, W., Rall, B. C., Brose, U. (2017). A general scaling law reveals why the largest animals are not the fastest. *Nat. Ecol. & Evol.* 1:8, 1116–22. doi: 10.1038/s41559-017-0241-4.

Horstkotte, T., Sandström, P., Neumann, W., Skarin, A., Adler, S., Roos, U., Sjögren, J. (2023). Semi-domesticated reindeer avoid winter habitats with exotic tree species *Pinus contorta*. Forest Ecology and Management, 540. doi: 10.1016/j.foreco.2023.121062

Houston, A. I. and McNamara, J. M. (2014). Foraging currencies, metabolism and behavioural routines. *J Anim Ecol*, 83: 30-40. doi: 10.1111/1365-2656.12096

Hudson, P. E., Corr, S. A., Payne-Davis, R. C., Clancy, S. N., Lane, E., Wilson, A. M. (2011). Functional anatomy of the cheetah (*Acinonyx jubatus*) hindlimb. *Journal of Anatomy* 218:4, 363–74. doi: 10.1111/j.1469-7580.2010.01310.x

Janzen, D. H. (1980). When is it coevolution. *Evolution,* 34:611–612.

Jeanniard-du-Dot, T., Guinet, C., Arnould, J. P. Y., Speakman, J. R. and Trites, A. W. (2017a). Accelerometers can measure total and activity-specific energy expenditures in free-ranging marine mammals only if linked to time-activity budgets. Funct Ecol, 31: 377-386. doi: 10.1111/1365-2435.12729

Jeanniard-du-Dot, T., Trites, A. W., Arnould, J. P. Y., Guinet, C. (2017b). Reproductive success is energetically linked to foraging efficiency in Antarctic fur seals. *PLoS One*. 12(4). doi: 10.1371/journal.pone.0174001

Jeanniard-du-Dot, T., Trites, A. W., Arnould, J. P. Y., Speakman, J. R., Guinet, C. (2017c). Activity-specific metabolic rates for diving, transiting, and resting at sea can be estimated from time–activity budgets in free-ranging marine mammals. *Ecol Evol.* 7: 2969–2976. doi: 10.1002/ece3.2546

Niven, J. E. and Laughlin, S. B. (2008). Energy limitation as a selective pressure on the evolution of sensory systems. *J Exp Biol.* 211(11):1792–1804. doi: 10.1242/jeb.017574

Jürgens, K. D., Bartels, H. and Bartels, R. (1981). Blood oxygen transport and organ weights of small bats and small non-flying mammals. *Respir Physiol*. 45(3):243-60. doi: 10.1016/0034-5687(81)90009-8

Kato, A., Ropert-Coudert, Y., Gremillet, D., Cannell, B. (2006). Locomotion and foraging strategy in foot-propelled and wing-propelled shallow-diving seabirds. *Mar. Ecol. Prog. Ser.* 308, 293–301.

Kearney, M. (2012). Metabolic theory, life history and the distribution of a terrestrial ectotherm. *Functional Ecology*, 26: 167-179. doi: 10.1111/j.1365-2435.2011.01917.x

King, J. R., and D. S. Farner. (1961). Energy metabolism, thermoregulation and body temperature. *Biology and Comparative Physiology of Birds*, Vol. 2 (A. L. Marshall, Ed.). London: Academic Press, p. 215.

Klappstein, N. J., Potts, J. R., Michelot, T., Börger, L., Pilfold, N. W., Lewis, M. A., Derocher, A. E. (2022). Energy-based step selection analysis: Modelling the energetic drivers of animal movement and habitat use. *J Anim Ecol.* 91(5):946-957. doi: 10.1111/1365-2656.13687

Kordas, R. L., Pawar, S., Kontopoulos, D. G., Woodward, G., O'Gorman, E. J. (2022). Metabolic plasticity can amplify ecosystem responses to global warming. *Nat Commun* 13, 2161. doi: 10.1038/s41467-022-29808-1

Kohles, J. E., O'Mara, M. T. and Dechmann, D. K. N. (2022). A conceptual framework to predict social information use based on food ephemerality and individual resource requirements. *Biol Rev*, 97: 2039-2056. doi: 10.1111/brv.12881

Ladds, M. A., Rosen, D. A. S., Slip, D. J. and Harcourt, R. G. (2017). Proxies of energy expenditure for marine mammals: an experimental test of "the time trap". *Sci Rep.* 7, 11815. doi: 10.1038/s41598-017-11576-4

Lescroël, A., Ballard, G., Toniolo, V., Barton, K. J., Wilson, P. R., Lyver, P. O. and Ainley, D. G. (2010). Working less to gain more: when breeding quality relates to foraging efficiency. *Ecology,* 91: 2044-2055. doi: 10.1890/09-0766.1

Lighton, J. R. and Halsey, L. G. (2011). Flow-through respirometry applied to chamber systems: pros and cons, hints and tips. *Comp Biochem Physiol A Mol Integr Physiol.* 158(3):265-75. doi: 10.1016/j.cbpa.2010.11.026

Madliger, C. L., Franklin, C. E. Love, O. P. and Cooke, S. J. (2020). Conservation Physiology: Applications for Wildlife Conservation and Management. *Oxford Academic*. Doi: 10.1093/oso/9780198843610.001.0001

Mandel, J. T. and Bildstein, K. L. (2007). Turkey Vultures Use Anthropogenic Thermals to Extend Their Daily Activity Period. *The Wilson Journal of Ornithology*, 119(1), 102–105.

Martins, G. (2024). The Metabolic Theory of Ecology as a Mechanistic Approach. In: *New Mechanism. History, Philosophy and Theory of the Life Sciences*, 35. *Springer, Cham*. doi: 10.1007/978-3-031-46917-6_3

Masello, J. F., Barbosa, A., Kato, A., Mattern, T., Medeiros, R., Stockdale, J. E., et al. (2021). How animals distribute themselves in space: energy landscapes of Antarctic avian predators. *Mov Ecol.* 9, 24. doi: 10.1186/s40462-021-00255-9

McCracken, G. F. & Bradbury J. W. (1977). Paternity and genetic heterogeneity in the polygynous bat, *Phyllostomus hastatus*. *Science* 198, 303-306.

McCracken, G. F. & Bradby J. W. (1981). Social organization and kinship in the polygynous bat *Phyllostomus hastatus*. *Behav. Ecol. Sociobiol.* 8, 11-34.

McInnes, A. M., McGeorge, C., Ginsberg, S., Pichegru, L. and Pistorius, P. A. (2017). Group foraging increases foraging efficiency in a piscivorous diver, the African penguin. *R. Soc. Open Sci.* 4170918 doi: 10.1098/rsos.170918

McNab, B. K. and Weston, K. A. (2018). The energetics of torpor in a temperate passerine endemic to New Zealand, the Rifleman (*Acanthisitta chloris*). *Journal Comp Physiol,* 360 B 188:855-862

McGrosky, A. & Pontzer, H. (2023). The fire of evolution: energy expenditure and ecology in primates and other endotherms. *J Exp Biol*. 226 (5). doi: 10.1242/jeb.245272

Meachen, J., Schmidt-Küntzel, A., Haefele, H., Steenkamp, G., Robinson, J. M., Randau, M., et al. (2018). Chapter 7 Cheetah specialization: Physiology and Morphology. *Cheetahs: Biology and Conservation: Biodiversity of the World: Conservation from Genes to Landscapes.* 93-105. doi: 10.1016/B978-0-12-804088-1.00007-1

Metcalfe, J.D., Wright, S., Tudorache, C. and Wilson, R.P. (2016). Recent advances in telemetry for estimating the energy metabolism of wild fishes. *J Fish Biol*, 88:284-297. doi: 10.1111/jfb.12804

Mills, M. G. L. and Mills, M. E. J. (2017). 'Energetics', Kalahari Cheetahs: Adaptations to an arid region. *Oxford Academic*. doi: 10.1093/oso/9780198712145.003.0008

Miwa, M., Oishi, K., Nakagawa, Y., Maeno, H., Anzai, H., et al. (2015) Application of Overall Dynamic Body Acceleration as a Proxy for Estimating the Energy Expenditure of Grazing Farm Animals: Relationship with Heart Rate. *PLOS ONE,* 10(6): e0128042. doi: 10.1371/journal.pone.0128042

Monteith, K. L., Stephenson, T. R., Bleich, V. C., Conner, M. M., Pierce, B. M., Bowyer, R. T. (2013). Risk-sensitive allocation in seasonal dynamics of fat and protein reserves in a long-lived mammal. *J Anim Ecol.* 82:377–88.

Monteith, K. L., Hayes, M. M., Kauffman, M. J., Copeland, H. E. and Sawyer, H. (2018). Functional attributes of ungulate migration: landscape features facilitate movement and access to forage. *Ecol Appl*, 28: 2153-2164. doi: 10.1002/eap.1803

Mori, T., Miyata, N., Aoyama, J. et al. (2015). Estimation of metabolic rate from activity measured by recorders deployed on Japanese sea bass *Lateolabrax japonicus*. *Fish Sci,* 81, 871–882. doi: 10.1007/s12562-015-0910-7

Nagy, K. A., Girard, I. A. & Brown, T. K. (1999). Energetics of Free-ranging Mammals, Reptiles, and Birds. *Annual Review of Nutrition*. 19:247-277. doi: 10.1146/annurev.nutr.19.1.247

Nathan, R., Getz, W. M., Revilla, E., Holyoak, M., Kadmon, R., Saltz, D., et al. (2008). A movement ecology paradigm for unifying organismal movement research. *Proc Natl Acad Sci.* 105(49):19052–9

Norberg, R. Å. (2021). To minimize foraging time, use high-efficiency, energy-expensive search and capture methods when food is abundant but low-efficiency, low-cost methods during food shortages. *Ecol Evol*. 11(23):16537-16546. doi: 10.1002/ece3.8204

Norberg, U. M. and Rayner J. M. V. (1987). Ecological morphology and flight in bats (Mammalia; Chiroptera): wing adaptations, flight performance, foraging strategy and echolocation. *Phil. Trans. R. Soc. Lond. B.* 316335–427 doi: 10.1098/rstb.1987.0030

O'Mara, T. M., Dechmann, D. D. K, Page, R. (2014). Frugivorous bats evaluate the quality of social information when choosing novel foods. *Behav. Ecol.*, 25, 1233–1239. doi: 10.1093/beheco/aru120

O'Mara, T. M., Wikelski, M., Voigt, C. C., Ter Maat, A., Pollock, H. S., Burness, G., et al. (2017). Cyclic bouts of extreme bradycardia counteract the high metabolism of frugivorous bats. *eLif* 6:e26686. doi: 10.7554/eLife.26686

O'Mara, T. M., Scharf A. K., Fahr, J., Abedi-Lartey, M., Wikelski, M., Dechmann, D. K. N., and Safi K. (2019). Overall Dynamic Body Acceleration in Straw-Colored Fruit Bats Increases in Headwinds but Not With Airspeed. *Front. Ecol. Evol.* 7:200. doi: 10.3389/fevo.2019.00200

O'Mara, M. T., Amorim, F., Scacco, M., McCracken, G. F., Safi, K., Mata, V., Tomé, R., Swartz, S., Wikelski, M., Beja, P., Rebelo, H., Dechmann, D. K. N. (2021). Bats use topography and nocturnal updrafts to fly high and fast. *Curr Biol*. 31(6):1311-1316.e4. doi: 10.1016/j.cub.2020.12.042

O'Mara, T. M. & Dechmann, D. K. N. (2023). Greater spear-nosed bats commute long distances alone, rest together, but forage apart. *Animal Behaviour*. 204, 37-48. doi: 10.1016/j.anbehav.2023.08.001

Page, R. & Ryan, M. (2006). Social transmission of novel foraging behavior in bats: frog calls and their referents. *Curr. Biol.*, 16(12), 1201–1205. doi: 10.1016/j.cub.2006.04.038

Qasem, L., Cardew, A., Wilson, A., Griffiths, I., Halsey, L. G., et al. (2012). Tri-Axial Dynamic Acceleration as a Proxy for Animal Energy Expenditure; Should We Be Summing Values or Calculating the Vector?. *PLOS ONE.* 7(2): e31187. doi: 10.1371/journal.pone.0031187

Parker, K. L., Gillingham, M. P., Hanley, T. A. and Robbins. C. T. (1996). Foraging efficiency: energy expenditure versus energy gain in free-ranging black-tailed deer. *Canadian Journal of Zoology.* 74(3): 442-450. doi: 10.1139/z96-051

Patterson, A., Gilchrist, H. G., Chivers, L., Hatch, S., Elliott, K. (2019). A comparison of techniques for classifying behavior from accelerometers for two species of seabird. *Ecol Evol.* 9: 3030–3045. doi: 10.1002/ece3.4740

Payne, N. L., Snelling, E. P., Fitzpatrick, R., Seymour, J., Courtney, R., Barnett, A. et al. (2015). A new method for resolving uncertainty of energy requirements in large water breathers: the ‘mega-flume' seagoing swim-tunnel respirometer. *Met Ecol, Evol* 6: 668-677.

Pennycuick, C. J. (2008). Modelling the Flying Bird. London: Academic Press.

Pennycuick, C. J. (1975). Mechanics of flight. *Avian Biology*, 5(1), 1-75.

Pontzer, H. and McGrosky, A. (2022). Balancing growth, reproduction, maintenance, and activity in evolved energy economies. *Current Biology*, 32(12):R709-R719. doi: 10.1016/j.cub.2022.05.018.

Ramakers, J. J. C., Dechmann, D. K. N., Page, R. A., O’Mara, M. T. (2016). Frugivorous bats prefer information from novel social partners. *Anim. Behav*. 116, 83–87. doi: 10.1016/j.anbehav.2016.03.021

Rayner, J. M. V. (1979). A New Approach to Animal Flight Mechanics. *J. Exp. Biol.* 80(1), 17–54. doi: 10.1242/jeb.80.1.17

Ratcliffe, J. & ter Hofstede, H. (2005). Roosts as information centres: social learning of food preferences in bats. *Biol. Lett.*, 1(1), 72–74. doi: 10.1098/rsbl.2004.0252

Rebstock, G. A., Abrahms, B. and Boersma, P. D. (2022). Site fidelity increases reproductive success by increasing foraging efficiency in a marine predator. *Behav Ecol*, 33(4), 868–875. doi: 10.1093/beheco/arac052

Reichle, D. E. (2023). Chapter 6 - Species adaptations to their energy environment. *The Global Carbon Cycle and Climate Change (Second Edition)*, *Elsevier*, 107-126. doi: 10.1016/B978-0-443-18775-9.00013-9

Rezende, G. C., Cruz-Neto, A. P., Borger, L., Redcliffe, J., Hambly, C., Speakman, J. R. *et al*. (2023). Validating Dynamic Body Acceleration metrics as a measure of energy expenditure in a Neotropical primate. *bioRxiv*, 2023-06.

Riskin, D. K., Iriarte-Diaz, J., Middleton, K. M., Breuer, K. S., and Swartz, S. M. (2010). The effect of body size on the wing movements of pteropodid bats, with insights into thrust and lift production. *J. Exp. Biol.* 213(23), 4110–4122. doi: 10.1242/jeb.043091

Robertson, G. S., Bolton, M. and Monaghan, P. (2016). Influence of diet and foraging strategy on reproductive success in two morphologically similar sympatric seabirds. *Bird Study*, 63(3), 319–329. doi: 10.1080/00063657.2016.1183112

Sabat, P., Bozinovic, F. and Zambrano, F. (1995). Role of dietary substrates on intestinal disaccharidases, digestibility, and energetics in the insectivorous mouse-opossum (*Thylamys elegans*). *Journal of Mammalogy*, 76(2), 603-611

Sansom, A., Lind, J. and Cresswell, W. (2009). Individual behavior and survival: the roles of predator avoidance, foraging success, and vigilance. *Behavioral Ecology*, 20(6):1168–1174. doi: 10.1093/beheco/arp110

Scales, J. A., A. A. King, and M. A. Butler. (2009). Running for your life or running for your dinner: what drives fiber-type evolution in lizard locomotor muscles? *Am. Nat.* 173: 543–553.

Scacco, M. (2021). On the role of topography and atmospheric conditions to support efficient movement: How flying animals use the energy in the landscape to travel efficiently. (*Doctoral dissertation, Konstanz*).

Scacco, M., Flack, A., Duriez, O., Wikelski, M., Safi, K. (2019). Static landscape features predict uplift locations for soaring birds across Europe. *R. Soc. Open Sci.* 6:1. doi: 10.1098/rsos.181440

Schramski, J. R., Dell, A. I., Grady, J. M., Sibly, R. M., Brown, J. H. (2015). Metabolic theory predicts whole-ecosystem properties. *Proc Natl Acad Sci U S A.* 112(8):2617-22. doi: 10.1073/pnas.1423502112

Shaw, A. K. (2020). Causes and consequences of individual variation in animal movement. Mov Ecol 8, 12. doi: 10.1186/s40462-020-0197-x

Shepard, E. L. C., Wilson, R. P., Quintana, F., Laich, A. G., Liebsch, N., Albareda, D. A., et al. (2008). Identification of animal movement patterns using tri-axial accelerometry. *Mov. Ecol.* 5:6, doi: 10.3354/esr00084

Shepard, E. L. C., Wilson, R. P., Rees, W. G., Grundy, E., Lambertucci, S. A., Vosper, S. B. (2013). Energy Landscapes Shape Animal Movement Ecology. *Am Nat.* 182:3, 298-312. doi: 10.1086/671257

Shepard, E. L. C., Ross, A. N., Portugal, S. J. (2016). Moving in a moving medium: new perspectives on flight. *Phil. Trans. R. Soc. B.* 371:1704. doi: 10.1098/rstb.2015.0382

Snijders, L., Krause, S., Tump, A. N., Breuker, M., Ortiz, C., Rizzi, S. et al. (2021). Causal evidence for the adaptive benefits of social foraging in the wild. *Commun Biol,* 4(94). doi: 10.1038/s42003-020-01597-7

Simpson, G. G. (1944). Tempo and mode in evolution. *Columbia Univ. Press, New York.*

Smallegange, I. M., Caswell, H., Toorians, M. E. M. de Roos, A. M. (2017). Mechanistic description of population dynamics using dynamic energy budget theory incorporated into integral projection models. *Methods Ecol Evol*. 8: 146-154. doi: 10.1111/2041-210X.12675

Speakman, J. R. (1997). Doubly-labelled water: theory and practice. *Chapman and Hall.*

Speakman, J. R. and Racey, P. A. (1988). The doubly-labelled water technique for measurement of energy expenditure in free-living animals. *Science Progress*, 72(286), 227–237.

Stearns, S. C. (1998). The evolution of life histories. *Oxford university press*.

Stephens, D. W. and Krebs, J. R. (1986). Foraging Theory (Vol. 1). *Princeton University Press*. doi: 10.2307/j.ctvs32s6b

Stothart, M. R., Elliott, K. H., Wood, T., Hatch, S. A., Speakman, J. R. (2016). Counting calories in cormorants: dynamic body acceleration predicts daily energy expenditure measured in pelagic cormorants. *J. Exp. Biol*. 219(14), 2192-2200. doi: 10.1242/jeb.130526

Sutton, G. J., Angel, L. P., Speakman, J. R., Arnould, J. P. Y. (2023). Determining energy expenditure in a large seabird using accelerometry. *J Exp Biol.* 226(23) doi: 10.1242/jeb.246922

Sutton, G. J., Botha, J. A., Speakman, J. R., Arnould, J. P. Y. (2021). Validating accelerometry-derived proxies of energy expenditure using the doubly labelled water method in the smallest penguin species. *Biol Open*, 10 (4): bio055475. doi: 10.1242/bio.055475

Thomas, S. P. & Suthers, R. A. (1972). The Physiology and Energetics of Bat Flight. *J Exp Biol* 57(2): 317–335. doi:10.1242/jeb.57.2.317

Tobalske, B. W., Hedrick, T. L., Dial, K. P., Biewener, A. A. (2003). Comparative power curves in bird flight. *Nature,* 421, 363–366. doi: 10.1038/nature01284

Toledo, S., Shohami, D., Schiffner, I., Lourie, E., Orchan, Y., Bartan, Y., and Nathan, R. (2020). Cognitive map-based navigation in wild bats revealed by a new high-put tracking system. *Science,* 369(6500), 188e193. doi: 10.1126/science.aax6904

Tomlinson, S., Arnall, S. G., Munn, A., Bradshaw, S. D., Maloney, S. K., Dixon, K. W., Didham, R. K. (2014). Applications and implications of ecological energetics. *Trends Ecol Evol*. 29(5):280-90. doi: 10.1016/j.tree.2014.03.003

Tucker, V. A. (1974). Energetics of natural avian flight. *Avian Energetics (R.A. Paynter, Ed)*. 298-334.

Udyawer, V., Simpfendorfer, C. A., Heupel, M. R. and Clark, T. D. (2017). Temporal and spatial activity-associated energy partitioning in free-swimming sea snakes. *Functional Ecology*, 31(9), 1739–1749.

von Busse, R., Waldman, R. M., Swartz, S. M., Voigt, C. C. and Breuer, K. S. (2014). The aerodynamic cost of flight in the short-tailed fruit bat (*Carollia perspicillata*): comparing theory with measurement. *J. R. Soc. Interface.* 1120140147. doi: 10.1098/rsif.2014.0147

Wang, Y., Smith, J. A. and Wilmers, C. C. (2017). Residential development alters behavior, movement, and energetics in an apex predator, the puma. *PLoS ONE,* 12(10): e0184687. doi: 10.1371/journal.pone.0184687

Watanabe, Y. Y., Ito, K., Kokubun, N. and Takahashi, A. (2020). Foraging behavior links sea ice to breeding success in Antarctic penguins. *Sci. Adv*. 6. doi: 10.1126/sciadv.aba4828

Ward, S., Möller, U., Rayner, J. M. V., Jackson, D. M., Bilo, D., Nachtigall, W., Speakman, J. R. (2001). Metabolic power, mechanical power and efficiency during wind tunnel flight by the European starling *Sturnus vulgaris*. *J. Exp. Biol*. 204, 3311-3322. doi: 10.1242/jeb.204.19.3311

Weimerskirch, H., Ancel, A., Caloin, M., Zahariev, A., Spagiari, J., Kersten, M., and Chastel, O. (2003). Foraging efficiency and adjustment of energy expenditure in a pelagic seabird provisioning its chick. *Journal of Animal Ecology*, *72*(3), 500-508. doi: 10.1046/j.1365-2656.2002.00720.x

Weimerskirch, H., Bishop, C., Jeanniard-du-Dot, T., Prudor, A. and Sachs, G. (2016). Frigate birds track atmospheric conditions over months-long transoceanic flights. *Science*, 353:74-78. doi: 10.1126/science.aaf4374

Westerterp, K.R. (2017). Doubly labelled water assessment of energy expenditure: principle, practice, and promise. *Eur J Appl Physiol,* 117, 1277–1285. doi: 10.1007/s00421-017-3641-x

Wikelski, M. and Cooke, S. J. (2006). Conservation physiology. *Trends in Ecology & Evolution,* 21(1):38-46. doi: 10.1016/j.tree.2005.10.018

Wilkinson G. S. & Boughman, W. J. (1998). Social calls coordinate foraging in greater spear-nosed bats. *Anim Behav*. 55(2):337-50. doi: 10.1006/anbe.1997.0557

Wilkinson, G. S., Carter, G. G., Bohn, K. M., Adams, D. M. (2016). Non-kin cooperation in bats. *Phil. Trans. R. Soc. B.* 371. doi: 10.1098/rstb.2015.0095

Williams, T. M., Dobson, G. P., Mathieu-Costello, O., Morsbach, D., Worley, M. B., Phillips, J. A. (1997). Skeletal muscle histology and biochemistry of an elite sprinter, the African cheetah. *J. Comp. Physiol. B.*167(8), 527-35. doi: 10.1007/s003600050105

Williams, T. M., Wolfe, L., Davis, T., Kendall, T., Richter, B., Wang, Y., et al. (2014). Instantaneous Energetics of Puma Kills Reveal Advantage of Felid Sneak Attacks. *Science* 346(6205), 81–85. doi: 10.1126/science.1254885

Williams, H. J. and Safi, K. (2021). Certainty and integration of options in animal movement. *Trends Ecol. Evol.* 36:11, 990-999. doi: 10.1016/j.tree.2021.06.013

Wilson, A. M., Lowe, J. C., Roskilly, K., Hudson, P. E., Golabek, K. A. and McNutt, J. W. (2013). Locomotion dynamics of hunting in wild cheetahs. *Nature*, 498(7453):185-189.

Wilson, A., Hubel, T., Wilshin, S. et al. (2018). Biomechanics of predator–prey arms race in lion, zebra, cheetah and impala. *Nature,* 554, 183–188. doi: 0.1038/nature25479

Wilson, R. P., White, C. R., Quintana, F., Halsey, L. G., Liebsch, N., Martin, G. R, et al. (2006). Moving towards acceleration for estimates of activity-specific metabolic rate in free-living animals: the case of the cormorant. *J. Anim. Ecol.* 75, 1081–1090. doi:10.1111/j.1365-2656.2006.01127.x

Wilson, R. P., Quintana, F. and Hobson, V. J. (2012). Construction of energy landscapes can clarify the movement and distribution of foraging animals. *Proc. R. Soc. B.* 279975–980 doi: 10.1098/rspb.2011.1544

Wilson, R. P., Börger, L., Holton, M. D., Scantlebury, D. M., Gómez-Laich, A., Quintana, et al. (2020). Estimates for energy expenditure in free-living animals using acceleration proxies: A reappraisal. *Journal of Animal Ecology*, *89*(1), 161–172. doi: 10.1111/1365-2656.13040

Wright, G. S. (2016). Social Learning and Information Transfer in Bats: Conspecific Influence Regarding Roosts, Calls, and Food. *Sociality in Bats*, 211–230.

Wright, S., Metcalfe, J. D., Hetherington, S. and Wilson, R. (2014). Estimating activity-specific energy expenditure in a teleost fish, using accelerometer loggers. *Marine Ecology Progress Series*, 496, 19–32.